JGR Oceans

RESEARCH ARTICLE
10.1029/2020JC016810

Special Section:
Coastal hydrology and oceanography

Key Points:

- Computation of coastal flooding in the Mahanadi delta is carried out by incorporating the river systems in the computational domain
- Contribution of upstream discharge is quantified for the 1999 Super cyclone
- Quantification of cyclone induced precipitation on simulation of coastal inundation using coupled model system of Advanced Circulation and Hydrologic Engineering Center River Analysis System

Correspondence to:
S. Pandey,
smita.itsme@gmail.com

Citation:
Pandey, S., Rao, A. D., & Haldar, R. (2021). Modeling of Coastal inundation in response to a tropical cyclone using a coupled hydraulic HEC-RAS and ADCIRC model. *Journal of Geophysical Research: Oceans*, *126*, e2020JC016810. https://doi.org/10.1029/2020JC016810

Received 18 SEP 2020
Accepted 4 JUN 2021

Modeling of Coastal Inundation in Response to a Tropical Cyclone Using a Coupled Hydraulic HEC-RAS and ADCIRC Model

Smita Pandey[1], A. D. Rao[1], and Raktim Haldar[2]

[1]Centre for Atmospheric Sciences, Indian Institute of Technology Delhi, New Delhi, India, [2]Department of Civil Engineering, Indian Institute of Technology Delhi, New Delhi, India

Abstract Coastal flooding as a combined effect of storm-tides, river discharge (RD) and rainfall during a cyclone period is of a major concern, particularly, in the river delta regions. The low-lying Mahanadi river delta located in the maritime state of Odisha along the east coast of India is highly prone to inland flooding due to any impinging cyclone in the region. Hence, computation of coastal flooding is seen for the 1999 Super cyclone and the 2013 Phailin cyclone using a standalone Advanced Circulation (ADCIRC) and a coupled Hydrologic Engineering Center River Analysis System and ADCIRC model. The Mahanadi, Brahmani, and Baitarani rivers are included in the computational domain with representative depths based on available river cross-sectional data. The model simulations infer that inundated coastal area is enhanced by 64% after representing the river delta in the domain, while the RD from the upstream contributes an additional 14%. The effect of RD and the role of land use/land cover on the computation of flooding during the 1999 Super cyclone is also investigated. The coupled system is used to quantify the contribution of precipitation on inland flooding during the cyclone period. The results signify that the inundated area becomes almost double after including rainfall data in both the cyclonic events. Also, the model generated inundated area during the Phailin cyclone is in a better match with the satellite image, demonstrating the coupled system can simulate a reliable inland flooding in the delta region. It concludes further that it is essential to resolve the river systems and incorporate hydrological components, like RD and precipitation for precise computation of inundation.

Plain Language Summary Tropical cyclone induced coastal flooding is the reoccurring disaster in the low-lying coastal regions. The risk of coastal inundation in the region increases with storm-tide interaction with the river systems and the intense precipitation during the cyclone period. The vulnerability enhances particularly, if the cyclone makes landfall near the estuaries, river deltas, or any adjoining rivers in the coastal area. Therefore, it is important to understand their interaction and quantify their contribution to coastal inundation for precise mapping of inland flooding. In this study, numerical simulations are performed for the 1999 Super cyclone and the Phailin cyclone using a standalone Advanced Circulation (ADCIRC) and a coupled system of ADCIRC and Hydrologic Engineering Center River Analysis System model for understanding the contribution of storm-tides, river discharge, and cyclone induced precipitation on simulation of coastal flooding. The simulations suggest that a coupled model with a properly resolved river system and hydrological components like river discharge and precipitation helps to achieve more detailed flood mapping in the river delta region.

1. Introduction

Coastal inundation associated with tropical cyclones is one of the main factors, which leads to destruction along the coast. It is fundamental to understand the contribution of tides, surges, river discharge (RD), and inland rainfall (P) on coastal inundation by representing the river deltaic region more accurately. When the storm tides (STs) penetrate through the downstream of the river and interact with the freshwater discharge from the river upstream, it enhances the flood risk by inundating larger areas along the river banks (Bacopoulos et al., 2017). The combined effect of surges and tides hereafter is referred as ST. River characteristics such as its depth, width, meandering, bed slope, and location of the river mouth with respect to the cyclone tracks are some factors that determine the role of the river basin for inland flooding. Therefore, accurately representing the river system in hydrodynamic models is essential to understand flood risk (Bunya et al., 2010; Peng et al., 2004; Westerink et al., 2008).

Several studies (Bhaskaran et al., 2013; Murty et al., 2014; Poulose et al., 2018; Rao et al., 2013, 2020) signify the importance of tide-surge interaction for accurate prediction of ST and coastal inundation. However, the importance of hydrological components like RD and P are also mentioned in the studies of Tromble et al. (2010). Thus, to precisely delineate coastal inundation and predict accurate water levels, a prediction system is needed that incorporates a combined hydrological and hydrodynamic approach. Some studies suggest the importance of this system in a real-time forecast (Beardsley et al., 2013; Dresback et al., 2013; Georgas et al., 2016; Van Cooten et al., 2011).

Studies by Westerink et al. (2008), Bunya et al. (2010) and Dietrich et al. (2011) used basin to channel scale unstructured Advanced Circulation (ADCIRC) model with hydrological component. They emphasized on the use of high-resolution complex overland features to simulate riverine flows, tides and storm surges. Tromble et al. (2010, 2013) used offline coupling of hydrological models, with unstructured ADCIRC model to compute hurricane storm surge induced inundation. Dresback et al. (2013) developed a one-way coupled hydrological and hydrodynamic model for real-time forecast scenarios. The model was tested during the passage of Hurricane Irene in North Carolina. The hydrological model in the coupled system considered both observed and forecasted precipitation in the upstream of the river boundary. However, rainfall below the upstream boundary was neglected in the study. It concluded that freshwater discharge had a negligible effect on the total water levels for Hurricane Irene.

Zheng et al. (2013) investigated the dependence between extreme rainfall and storm surge in determining flood-risk along the Australian coastline using statistical simulations. Their model used observational records of P and storm events. They showed that the strength of dependence varies with the lag between the events and storm burst duration. The study made an emphasis that extreme P and storm surges must be considered together if inland inundation is to be quantified correctly. Ray et al. (2011) carried out dynamical hydraulic modeling using the 1D Hydrologic Engineering Center River Analysis System (HEC-RAS) model for steady and unsteady states to analyze the combined effect of storm surges and P in the Houston area. They found that storm surges timing with respect to P plays a vital role in coastal flooding. Recently, Pasquier et al. (2019) assessed a coastal region's sensitivity to different sources of flooding using HEC-RAS version 5.0. They showed that flooding due to storm surges can be exacerbated by the high discharge and must incorporate hydrological conditions occurring during the events to evaluate flood-risk.

Very few studies for the Indian coast (Agnihotri et al., 2006; Dube et al., 2005; Sinha et al., 2008) are carried out in the past that have looked at river-tide-surge interaction using finite-difference grid but failed in the representation of river systems accurately. Recently, Gayathri et al. (2019) demonstrated river-tide-surge interaction by incorporating idealized hydrological components for the Hooghly River in the hydrodynamic ADCIRC model. They signify that the limit of flood flow penetration varies from 70 to 62 km for a minimum discharge of 1000 m^3/s to a maximum discharge of 3000 m^3/s, respectively. They also investigated role of the wind stress by taking hypothetical Aila cyclone and the discharge on surge propagation and reported that lower discharge with higher wind stress results in a more considerable extent of surge penetration. However, the study did not discuss the river-induced flooding during the cyclone period as the river channel had an idealized bathymetry, which may accumulate enough water without causing overbank flooding.

The above studies show the importance of accurate representation of geographical features and incorporation of the hydrological component, including RD and cyclone induced P, to compute coastal flood levels during cyclonic events. However, due to the lack of availability of detailed river bathymetry and other hydrological data, it is still a challenge to understand the contribution of the hydrological factors responsible for inland flooding during the cyclonic events. The Indian coast, particularly the east coast of India, is frequently affected by landfalling cyclones (http://www.imd.gov.in). Many Indian river systems such as Godavari, Krishna, Mahanadi, Brahmani, Baitarani, and Hooghly join the Bay of Bengal (BoB).

According to the India Meteorological Department report (IMD, 2018), Odisha is one of India's maritime states with more hazard-prone districts and highly susceptible to severe cyclonic storms. The Mahanadi River is one of the major river basins that flow in Odisha and empty into the BoB. The Mahanadi delta comprises a network of three rivers: The Mahanadi, the Brahmani, and the Baitarani (Kumar & Bhattacharya, 2003).

The Mahanadi River's catchment area is about 141,589 km^2, with 45% of it is in Odisha (Singh, 2017). The delta covers about 200 km long coastline extending from the Chilika lake in the south to the Dhamara River in the north. About 83% of the delta region is below 5 m contour and is vulnerable to floods as a consequence of any cyclone.

In the present work, a coupled modeling system is suggested by utilizing available data to a maximum extent for computation of coastal inundation as a combined effect of ST, RD and P. The Mahanadi, Brahmani and Baitarani rivers are included in the computational domain with representative depths. The system is corroborated by carrying out simulations for the 1999 Super cyclone and 2013 Phailin cyclone. The reason to consider these cyclonic cases for the study is that they made landfall into the delta region and to the south of it, respectively. The system is checked and validated for both the cases with the available data.

The experiments are carried out in two sections. Initially, hydrodynamic ADCIRC model is configured for the Odisha coast by incorporating all the three rivers as mentioned above. The field observed discharge during the cyclone period is taken as the upstream boundary condition in the model. The contribution of the inflow of freshwater discharge is also quantified. In contrast, the 2D unsteady state HEC-RAS model is configured for the Mahanadi delta in the second section, using daily RD as an upstream boundary and ADCIRC computed ST as a downstream boundary. Daily area-averaged P during the cyclone period is also considered to examine the coastal flooding, particularly in the river channel, as a response to the combined effect of ST, RD, and P.

This study is the first of its kind to compute coastal inundation for the Indian coast by incorporating the effect of precipitation along with the other principal components such as storm surges, tides and RD during the cyclone period. The earlier studies carried out for Indian region either failed to represent the river systems or carried out using unrealistic bathymetry and RD data, which made it difficult to study the inland flooding as a compound effect of RD and ST. The modeling system suggested in the present study helps to understand and quantify the contribution of hydrological components during any cyclonic event

2. Synoptic History of Cyclones

2.1. 1999 Super Cyclone

The 1999 Super cyclone is the most intense tropical cyclone that crossed the Odisha coast. It is the most severe cyclone in the entire North Indian Ocean. The initial disturbance that led to this cyclone was noticed on October 24, 1999 in the Gulf of Thailand. While moving toward the west, it was emerged in the north Andaman Sea as a low-pressure system on October 25, 1999 and centered at 12.5°N/90.8°E. This system moved west northwesterly and intensified into a cyclonic storm (CS) on October 26. After strengthening into a severe cyclonic storm (SCS) on October 27, it was upgraded subsequently into a very severe cyclonic storm (VSCS) at 1500 UTC of October 27. Under favorable conditions, the storm intensified into a super cyclonic storm (SUCS) on October 28 and maintained its intensity as the system crossed Odisha coast near Paradeep between 0430 and 0630 UTC of October 29. The maximum pressure drop for the cyclone was 98 hPa, and the maximum sustained wind speed of about 72 m/s. After crossing the coast, the system weakened into a VSCS and tracked slowly toward northwest near Cuttack. The generated storm surge of about 8–9 m was reported in the Regional Specialized Meteorological Center (RSMC) report (RSMC, 1999) and high flood, particularly in Baitarani and Brahmani (Kalsi & Srivastava, 2006). According to the report, the cyclone caused severe damage in Jagatsinghpur, Kendrapara, Jajpur, Puri, Bhadrak, Khurda, Dhenkanal, Balasore, Keonjhar, Nayangarh, and Cuttack districts of Odisha. The 1999 Super cyclone caused more than 10,000 fatalities in Odisha, and the vulnerability was higher in the Mahanadi river basin (Chittibabu et al., 2004; Dube et al., 2005).

2.2. Phailin Cyclone

The VSCS Phailin in 2013 was the second strongest tropical cyclone to make landfall near Gopalpur in Odisha coast after the 1999 Super cyclone (RSMC, 2013). On October 8, 2013, at 0300 UTC, a depression (D) was formed over the North Andaman Sea and moved northwestward with a speed of 13 km/h. The deep depression (DD) was intensified into a CS on 9 October. The cyclone further moved westward and intensified into

Table 1
Cyclone Track Information for 1999 Super Cyclone and 2013 Phailin Cyclone

1999 Super cyclone				2013 Phailin cyclone			
Date	Latitude	Longitude	Intensity	Date	Latitude	Longitude	Intensity
October 25, 1999	12.0	98.5	D	October 08, 2013	12.0	96.0	D
October 26, 1999	13.5	95.0	CS	October 09, 2013	13.0	93.5	DD
October 27, 1999	16.0	92.0	SCS	October 10, 2013	15.0	90.5	VSCS
October 27, 1999	17.0	90.5	VSCS	October 11, 2013	16.0	88.5	ESCS
October 28, 1999	19.0	87.5	SUCS	October 12, 2013	17.5	86.5	ESCS
October 29, 1999	20.5	86.0	SUCS				

Abbreviations: D, Depression; DD, deep depression; CS, cyclonic storm; ESCS, extreme severe cyclonic storm; SCS, severe cyclonic storm; SUCS, super cyclonic storm; VSCS, very severe cyclonic storm.

a VSCS on 10 October at 0600 UTC and finally crossed the Odisha coast near Gopalpur around 1700 UTC on October 12 as an extreme severe cyclonic storm. The maximum pressure drop of the cyclone was 66 hPa and the maximum sustained wind speed was around 60 m/s. A storm surge of about 3–3.5 m and inundation in the low-lying areas of Ganjam, Puri, and Jagatsinghpur districts of Odisha was reported by IMD. Improved prediction of Phailin cyclone by IMD helped to reduce the fatalities during the event. Table 1 gives the best track information of the cyclones and the intensity indicated in the table is taken from IMD (http://www.rsmcnewdelhi.imd.gov.in/images/pdf/faq.pdf). Figure 1 shows the computational domain along with the 1999 Super cyclone and the 2013 Phailin cyclone tracks.

3. Model Description

3.1. ADCIRC Formulation

The US Army Corps of Engineers, Engineering Research and Development Center, University of Notre Dame, and the University of North Carolina jointly developed a finite element based hydrodynamic model

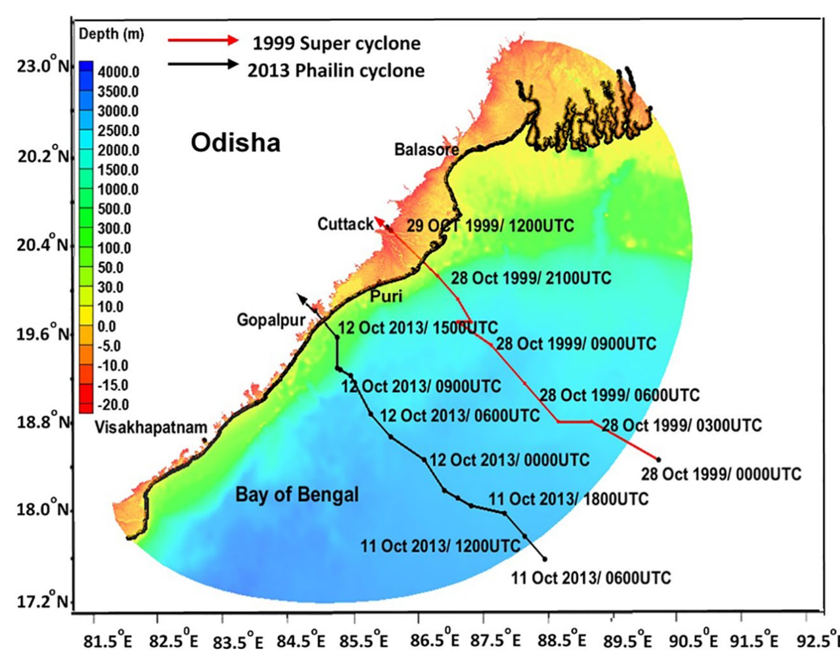

Figure 1. Model domain along with 1999 Super cyclone (in red) and 2013 Phailin cyclone (in black) tracks.

ADCIRC. The model uses a highly flexible, unstructured grid to solve fully non-linear shallow water equations (SWEs) with the Boussinesq and hydrostatic approximations (Luettich et al., 1992). The ADCIRC can be utilized to simulate time-dependent, free-surface circulation in a two-dimensional (2D) depth-integrated mode or a three-dimensional (3D) model. The model solves the generalized wave continuity equation (GWCE) (Kinnmark, 1986) to obtain the elevation changes and the momentum equations for the currents (Luettich & Westerink, 2004). For the GWCE, the model uses a semi-implicit, three-time level approximation. However, in the momentum equation, fully explicit mode, two-time level approximation is used. It also uses Galerkin finite element method in space, and at the same time, GWCE provides stability to the model by eliminating any spurious oscillations associated with the technique (Atkinson et al., 2004; Dawson et al., 2006; Kolar et al., 1994; Luettich & Westerink, 2004). The developments in the equations and expansion of the model can be found in Kinnmark (1986), Luettich et al. (1992), and Kolar et al. (1994).

The ADCIRC includes different boundary conditions (Luettich & Westerink, 2004) like free-surface elevation from different tidal constituents at the open boundary and normal flux per unit width (zero flux across the land boundary and non-zero flux across the river) at the flux boundary. The later boundary condition is used to represent river inflow by specifying RD into the model domain. It helps in simulating the river flow and its interaction with ST. For a more accurate representation of the bottom friction, the ADCIRC includes a quadratic parameterization of bottom stress using Manning's n formulation. The nodal value of Manning's n value is assigned spatially with the help of land use/land cover (LULC) data (Bunya et al., 2010). Inundation in the model is computed using the wetting and drying scheme (Dietrich et al., 2004; Luettich & Westerink, 2004).

3.2. HEC-RAS Formulation

HEC-RAS is developed by the HEC of the US Army Corps of Engineers (USACE, 2016). The HEC-RAS can be used either as a one dimensional (1D) steady or 1D and 2D unsteady flow model (Brunner, 2002). It can simulate hydraulic flow in river channels and flood plains in a single reach or a network of reaches. In the present study, the HEC-RAS version 5.0 is used as a 2D unsteady flow model. The 2D flow area is a closed domain divided into computation units, in which 2D unsteady flow equations are numerically solved. The 2D unsteady HEC-RAS model solves either the 2D SWEs or the diffusion wave approximation of the SWE with an implicit finite-volume algorithm on user selection. Hydrostatic pressure, incompressible flow, and uniform density are assumed for the formulation of the equations. The basic governing equations used in the model can be found in USACE (2016). The HEC-RAS model can be used with both unstructured and structured mesh. The model mesh can handle a polygon having a minimum of three sides (triangle) to maximum eight-sided (octagonal) computation cell. This model is well tested for coastal flood mapping as a combined effect of storm surge and P (Ray et al., 2011), fluvial flood (Patel et al., 2017; Quirogaa et al., 2016), and flooding driven by increased sea-level rise (Pasquier et al., 2019). However, its 2D capabilities are still required to be tested for different applications (Vozinaki et al., 2017).

4. Data and Methodology

4.1. ADCIRC

It is indispensable to represent the river system more specifically with all its important tributaries in the model domain for the computation of coastal flooding in the river basin as a combined effect of ST, upstream RD and inland P. Hence, the Mahanadi delta, comprising of the Mahanadi and the adjoining Brahmani, and Baitarani rivers, are digitized using Google Earth shown in Figures 2a and 2b. Once the rivers' land-water boundaries and its tributaries are digitized, it is converted into a polygon shapefile using geographic information system (GIS). Therefore, assigning bathymetry throughout the river polygon is a big challenge because it is not available in the public domain. However, the river cross-section data is available at five locations in the study area (Alipingal, Marshaghai, Pubansa, Indupur, and Jenapur) from the Water Resources Information System (WRIS) database (https://indiawris.gov.in/wris/#/). The year of availability of cross-sectional data for Jenapur and Pubansa is 2013 while, it is 2006 for Indupur, Marshaghai and Alipingal. The Shuttle Radar Topography Mission (SRTM) data (Farr et al., 2007) does not represent underwater elevation. Therefore, observed river cross-section data is used to assign river bed along the river

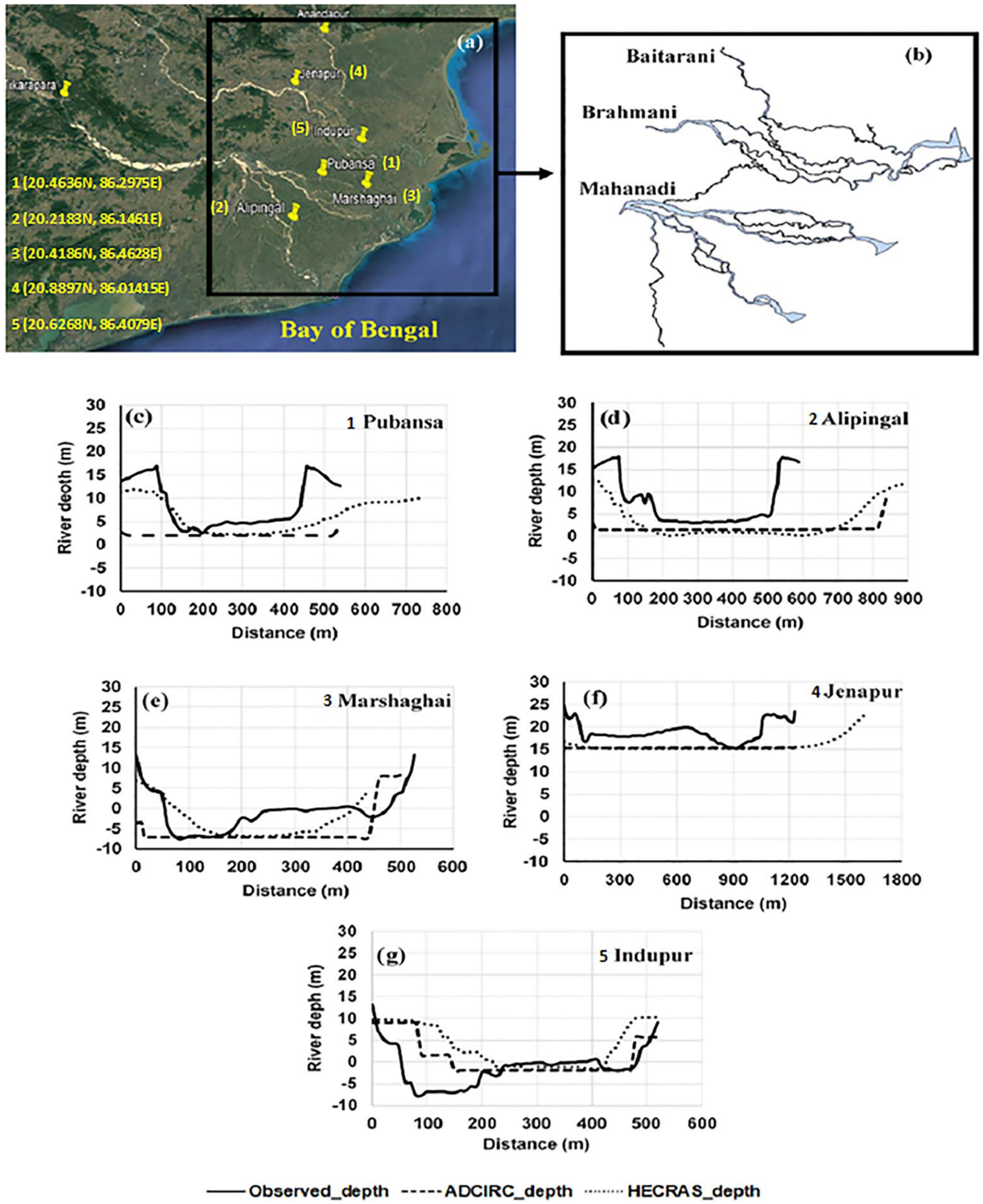

Figure 2. Depiction of (a) Mahanadi deltaic region along with river cross-sections and discharge observed locations (1–5) (b) Digitized Mahanadi, Brahmani, and Baitarani rivers along with their tributaries. Comparison of observed and computed Advanced Circulation and Hydrologic Engineering Center River Analysis System river cross-sectional depths along the river width at (c) Pubansa (d) Alipingal (e) Marshaghai (f) Jenapur (g) Indupur.

channels. The maximum cross-sectional depth of an observed locations (as shown in Figure 2a) in each stream is found and taken as a reference. This maximum depth is subtracted for the whole length of the river stream within the river boundary polygon, with reference to the river bank levels from the SRTM data using the Google Earth. This procedure is followed for all the river systems in the study domain. Later the river terrain with assigned river depth is used in place of general river terrain and merged with the surface terrain of SRTM data. This modified SRTM data (containing river channels with approximated depths) is used to generate regional mesh covering mostly the Odisha coast. The present study is an initial attempt to compute coastal inundation as a combined effect of ST, RD and P by approximating the bathymetry based on different sources of observations. Hence, the study is constrained by the availability of data. The model bathymetry is derived from the 30 arc-second General Bathymetric Chart of the Ocean (GEBCO) data (Weatherall et al., 2015). Figures 2c–2g depicts a comparison between the observed and model computed river cross-sectional depth. The river depth profile for the ADCIRC model is depicted as ADCIRC_depth. As the availability of the river cross-sectional profiles limited to few locations it is seen from the figure that the maximum depth of the river in the model matches reasonably well with the observations. While, the sensitivity experiments to assess the model uncertainties in computing inland inundation by changing the river cross-sectional width are described in Appendix C.

Mesh with an unstructured triangular grid is prepared using Surface Water Modeling System (SMS) (http://www.aquaveo.com/products) with 829,136 computational nodes. The resolution of the domain varies from minimum 50 m within the riverine region to maximum 23 km in the deeper ocean. The minimum cross-sectional width of the Mahanadi River in the domain is about 500 m and maximum of about 4,000 m. Whereas, in case of Brahmani and Baitarani rivers the maximum width is about 1500 and 700 m, respectively and the minimum is about 500 m for Brahmani and 200 m for Baitarani River. The extent of the inland boundary is up to 20 m topography contour, which allows having sufficient flood plains, and the normal inflow boundary for the Mahanadi, Brahmani, and Baitarani rivers is chosen at 16, 16, and 20 m, respectively. The offshore extent of the domain is about 484 km, and the open boundary is forced with amplitude and phase of 13 tidal constituents (K1, M2, N2, O1, P1, S2, K2, L2, 2N2, MU2, NU2, Q1, and T2) from the Le Provost tidal database (Le Provost et al., 1998). The present study uses two Digital Elevation Model (DEM) data one is the original 30 m SRTM and the other is the SRTM data modified using WRIS cross-sectional data. In order to study the effect of representing the river deltaic region on the coastal flooding, the topography of the computational domain is replaced by unmodified (original) 30 m SRTM data. Hereafter, the computational domain with modified SRTM data is referred to as DT-1, and it is DT-2 with the unmodified SRTM. The deltaic region of both the computational domain are shown in Appendix A.

Daily discharged data available at Tikarapara, Jenapur and Anandapur from WRIS during the simulation period is used at the upstream boundary of Mahanadi, Brahmani and Baitarani rivers, respectively in DT-1. In order to achieve a steady state, the model is spun-up for 30 days using tidal amplitude and corresponding phase of different constituents at the open boundary and daily discharge at the upstream flux boundary of the rivers. After the spin-up, the model is able to capture the complete tidal cycle, which is verified by validating model tides with observations available at tide gauge locations. Thereafter, the model is forced with the cyclonic winds during the storm period. The model simulations (DT-1 & DT-2) with the ADCIRC model are performed with a time-step of 0.5 s. Hybrid bottom friction formulation with minimum drag coefficient as 0.0015 is used in the computation of ST, when the LULC data is not considered. However, bottom friction is computed with LULC data by quadratic parametrization using Manning's *n* formulation. The formulation using Manning's *n* represent the surface roughness of different LULC types. The friction coefficient (Cf) is computed using

$$\mathrm{Cf}\left(\mathrm{t}\right) = \frac{\mathrm{g} * \mathrm{n}^2}{\left(h\left[+eta\left(t\right)\right]\right)^{1/3}}$$

where, *g* is the gravitational constant (9.81 m/s^2), *n* is the Manning's roughness coefficient, *h* is the bathymetric depth (m) and eta(*t*) is the water surface elevation (m) at time *t*.

Spatially varying Manning's *n* with 0.02 for open water and larger inland values based on LULC class are used for simulations with LULC data. In the present study, 1 km resolution of LULC data is obtained from sources of 2000 Global Land Cover Characterization (GLCC) and Bhuvan-National Remote Sensing Center (NRSC) 2013 LULC for the 1999 Super cyclone and Phailin cyclone, respectively. The table with value of Manning's *n* for different classes of LULC data used in the study is given in Appendix A. The value for Manning's *n* is obtained from the literature (Bricker et al., 2015; Bunya et al., 2010; Kalyanapu et al., 2009; Passeri et al., 2011; Phillips & Tadayon, 2006; Wamsley et al., 2009; Weltz et al., 1992).

In order to fix the values of the model parameters experiments were carried out using spatially constant horizontal eddy viscosity equals to 2 m^2/s and 50 m^2/s over the study domain. It was observed that for 2 m^2/s, the model was unstable and showed maximum elevation error in especially in narrow and meandering tributaries. However, in the present study, simulation of storm surges was not sensitive to the horizontal eddy viscosity variation in the ocean. Whereas, it was noticed that eddy viscosity plays a vital role in the upper stream of the tributaries such that the use of an higher value, 50 m^2/s is providing a stable

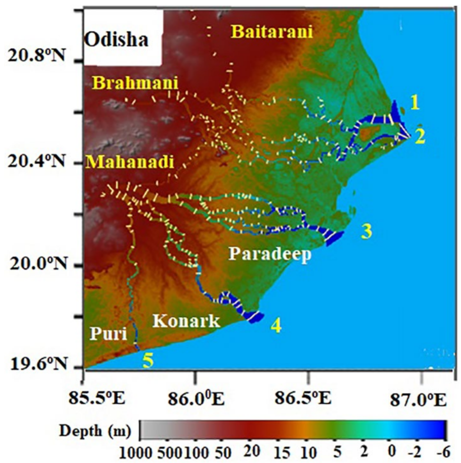

Figure 3. Computational domain for Hydrologic Engineering Center River Analysis System model along with cross-sections. Label 1–5 shows the river coast boundary openings for Baitarani, Brahmani, and the Mahanadi rivers, respectively.

solution. Therefore, the horizontal eddy viscosity is taken to be 2 m^2/s (Cyriac et al., 2018) in open waters (Pandey & Rao, 2019) and 50 m^2/s (Bunya et al, 2010) over the land. In the present study, the ramp function of 1 day is used based on the sensitivity experiments carried out on the computation of the inundated area as discussed in Appendix C. This value of 1 day ramp is also in accordance with the studies of Westerink et al. (1992), Shankar et al. (2019) and Blain et al. (1994). Typical values for the weighing factor (τ_0) in GWCE are in the range of 0.005–0.1. In the present study, the minimum and maximum value of tau0 is tested and it has resulted an unstable solution. However, $\tau_0 = 0.05$ gives realistic results, which is also used in Pandey and Rao (2019).

An improved dynamical Jelesnianski wind model (Jelesnianski & Taylor, 1973; Pandey & Rao, 2018) is used for cyclonic wind distribution. The information of cyclone position is obtained from the IMD best track data and the wind fields for both the cyclonic events are calculated by taking constant radius of maximum winds of 30 km, based on the observation of the past cyclones in this region (Mohapatra & Sharma, 2015; Sharma & Mohapatra, 2017).

4.2. HEC-RAS

For the computation of coastal flooding as the combined effect of ST, upstream discharge, and inland rainfall, a 2D hydraulic model for unsteady flow, is configured with the HEC-RAS (version 5.0) software. The study domain contains the Mahanadi delta region, and its elevation is taken from the modified 30 m SRTM data. RAS Mapper (the GIS extension of HEC-RAS) is used to manage and export model results. Cross-sections of the river channels are created at approximate intervals, taking care of locations where there is a sharp turning or change in the width of the rivers (Figure 3). The reason to take cross-sections at many locations is to specify the ground surface profile and specify the stream's flow carrying capacity and the adjacent flood plain. The cross-sectional depth profile of the river in the HEC-RAS model is compared with the observations from WRIS, as shown in Figures 2c–2g. It is seen from the figure that the depth profile of the HEC-RAS model, which is represented as HECRAS_depth is similar to the ADCIRC depth in terms of maximum depth, which is almost in close agreement with the observations. However, the river bank profile is modified in HEC-RAS using the cross-sectional data to create an improved river bank profiles for hydraulic modeling.

The flood plain in the HEC-RAS is represented by a series of cells called the storage area. The mesh size varies from 50 m within the river channel to 500 m in the floodplain. Water will flow into the storage area if the river level surpasses the corresponding height of the river bank. The computational domain covers an area of about 11728 km^2 with an upstream boundary near Cuttack, Jenapur, and Anandpur for the Mahanadi, Brahmani, and Baitarani rivers, respectively. The daily discharge data is taken from WRIS at Tikarapara, Jenapur, and Anandapur stations. At the same time, the ADCIRC simulated ST levels are taken at every 30 min interval at the downstream boundary of the domain. Daily rainfall gridded input with 25 km resolution is obtained from IMD (Pai et al., 2014). As the computational area is relatively small, daily area-averaged rainfall is used for model simulations. In the present study, the daily precipitation amounts are not disaggregated at sub-daily scale. However, the daily area-averaged precipitation time series is taken as input for model simulations and the model is integrated for a day using the daily precipitation. At present, the HEC-RAS modeling platform allows only time-varying precipitation within the computational domain. Hence, it is a limitation of the present study as it does not consider the spatial variation in precipitation over the river basin area. Table 2 shows the area-averaged precipitation (19.6–21.0°N and 85.0E-87.2°E) used in the HEC-RAS model for the simulation of the 1999 Super cyclone and Phailin cyclone. The simulations are carried out with a model time step of 60 s using the eddy viscosity transverse mixing coefficient as 2.0. The LULC data for Manning's n value is taken from the source mentioned in Section 3.1. Similar to the ADCIRC, the HEC-RAS model is initially run for 30 days with tides (computed from the ADCIRC) at the downstream boundary and daily observed discharge at the upstream boundary.

Table 2
Daily Area-Averaged Precipitation Over the Mahanadi Deltaic Region During 1999 Super Cyclone and Phailin Cyclone

1999 Super cyclone		2013 Phailin cyclone	
Day	Area-averaged precipitation (mm)	Day	Area-averaged precipitation (mm)
October 25, 1999	2.3	October 09, 2013	16.8
October 26, 1999	0	October 10, 2013	12
October 27, 1999	0.6	October 11, 2013	0.1
October 28, 1999	25.6	October 12, 2013	31
October 29, 1999	216.5	October 13, 2013	110
October 30, 1999	70.5		
October 31, 1999	5		

The 2D unsteady HEC-RAS model is used to simulate coastal flooding in response to the combined effect of ST, RD, and P in the Mahanadi delta region during the cyclone period. The experiments are carried out for both the 2013 Phailin and the 1999 Super cyclone. The first experiment (Exp1) is carried out by prescribing only ST (computed from the ADCIRC) and RD at downstream and upstream boundaries, respectively. At the same time, inland daily averaged rainfall over the domain is also included in the Exp2.

4.3. Coupling Methodology

In this study, computation of coastal inundation in the river deltaic region as a combined effect of P, RD and ST is carried out using a coupled 2D river hydraulic HEC-RAS model and hydrodynamic ADCIRC model. The two models are linked at the river coastal boundary (RCB) by one way coupling in which first simulations are performed to compute ST using standalone ADCIRC model. The opening locations of the RCB are shown in Figure 3 as they are labeled from 1-5 with Baitarani as 1, Brahmani 2, and 3–5 for Mahanadi River. Later, the ADCIRC computed ST levels are provided at the downstream boundary of the HEC-RAS model domain and daily river discharge data is taken at upper boundary. The daily rainfall is taken as the source flux term in the mass conservation equation of HEC-RAS to incorporate the effect of cyclone induced precipitation in flood inundation.

5. Results and Discussion

5.1. ADCIRC Simulations

5.1.1. 1999 Super Cyclone

Numerical simulations are carried out for the 1999 Super cyclone using the ADCIRC model to understand the role of upstream RD of the river delta on the coastal inundation. These cyclonic events are used to investigate the effect of landfall location on surge propagation and inland flooding in the region. The 1999 Super cyclone made landfall in the Mahanadi deltaic region, near Paradeep. To quantify the inland flooding in the Mahanadi delta during the 1999 Super cyclone, a simulation (SIM1) is first carried out with DT-1 taking cyclonic winds and tidal forcing along the open boundary. Tidal forcing is provided by specifying the amplitude and its phase of the important tidal constituents. A second simulation (SIM2) with DT-2 and the same experimental setup as that of SIM1 is made. Prior to these simulations, a steady state tidal solution is generated for DT-1 and DT-2 by integrating for about 30 days by prescribing only the tidal forcing at the open boundary.

Figures 4a and 4b depict the spatial coverage of coastal inundation and maximum water level (MWL) due to the 1999 Super cyclone computed from SIM1 & SIM2, respectively. The MWL of about 9 m is computed near the Brahmani River in SIM1. In contrast, the MWL of about 7 m is computed in SIM2, in the downstream of Mahanadi River. The MWL over the coastal region is estimated by subtracting the local topography as the model simulated water level is refered to the mean sea level. The extent of inundation in SIM1 is seen in some parts of Kendrapara, Jagatsinghpur, Bhadrak, and Jajpur districts. Moreover, the extent of coastal inundation is found upland up to 56 km near Brahmani River and 52 km near the Baitarani River. The extent of inundation is higher near the downstream of Brahmani and Baitarani rivers because these regions mainly experience on-shore cyclonic winds and subsequently the rivers in the region swelled over their banks, causing severe flooding in the adjacent coastal plains. The penetration of ST in the tributaries of Brahmani and Baitarani rivers are observed upto 40 km upstream from the coast. Moreover, the inundation noticed in the areas of Kendrapara and Jajpur districts is mainly caused due to overflow from the river banks. However in SIM2, only the storm waters at the river mouth penetrate through the river system and inundate the low-lying regions of Jagatsinghpur, Kendrapara, and Bhadrak with a maximum extent of inundation about 22, 16, and 17 km, respectively. The simulated inundated area is about 1,940 and 685 km^2 for SIM1 and SIM2, respectively. The inundated area in SIM1 increases by about 64% compared to SIM2.

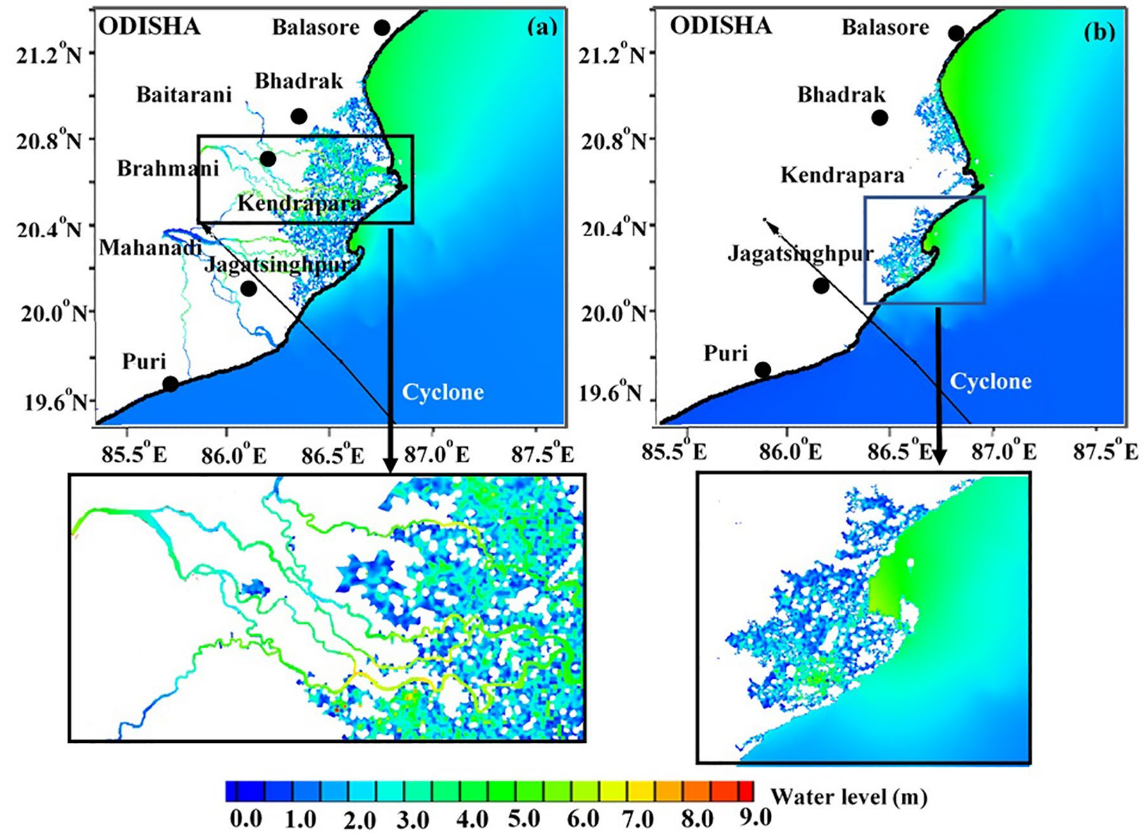

Figure 4. Spatial coverage of coastal inundation and maximum water levels for the 1999 Super cyclone (a) Domain with modified Shuttle Radar Topography Mission (SRTM) data (DT-1) (b) Domain with unmodified SRTM data (DT-2). Inset image is zoomed to highlight the area with maximum water levels in both the domains.

The increase may be attributed to the fact that the Mahanadi, Brahmani, and Baitarani rivers are represented with approximated depths in the computational domain (DT-1), and as the cyclone passes through the deltaic region, the strong on-shore cyclonic winds push the water through the river channel and causing inundation through the river banks. Comparison of SIM1 and SIM2 signifies the importance of proper representation of the river delta in the computation of inland inundation.

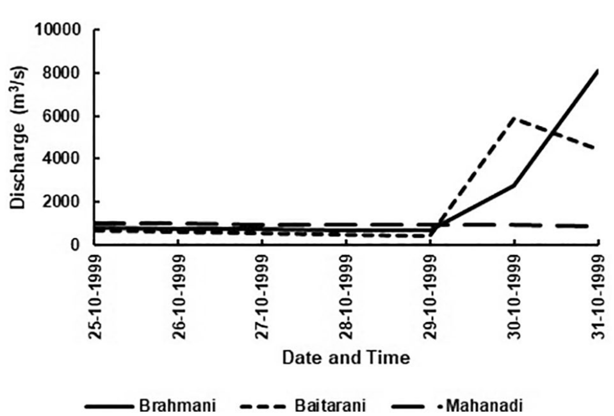

Figure 5. Daily discharge hydrograph during the 1999 Super cyclone at Mahanadi, Brahmani and Baitarani.

The effect of freshwater discharge on the inland flooding is assessed and quantified by performing another simulation (SIM3) with DT-1 considering tides along the open boundary, cyclonic winds, and daily discharge at the upstream of the Mahanadi, Brahmani, and Baitarani rivers. Initially, the DT-1 is forced with the tide and RD and spun-up the model for 30 days to reach a steady state. Later, the sea surface is forced by cyclonic winds to compute coastal inundation and MWL. Figure 5 shows the observed hydrograph for Mahanadi, Brahmani, and Baitarani rivers taken at Tikarapara, Jenapur, and Anandapur river locations, respectively, during the cyclone period. The effect of the RD on coastal flooding is analyzed by comparing SIM1 and SIM3. Spatial coverage of coastal inundation and MWL for SIM3 is shown in Figure 6a. A composite depiction of coastal inundation for the 1999 Super cyclone as an aggregate response of SIM1 and SIM3 is shown in Figure 6b. It is observed that there is no change in MWL after incorporating upstream discharge, however, the coastal inundation increases in the districts of Jajpur, Kendrapara, and Jagatsinghpur near Brahmani and Baitarani rivers. These districts are also mentioned in

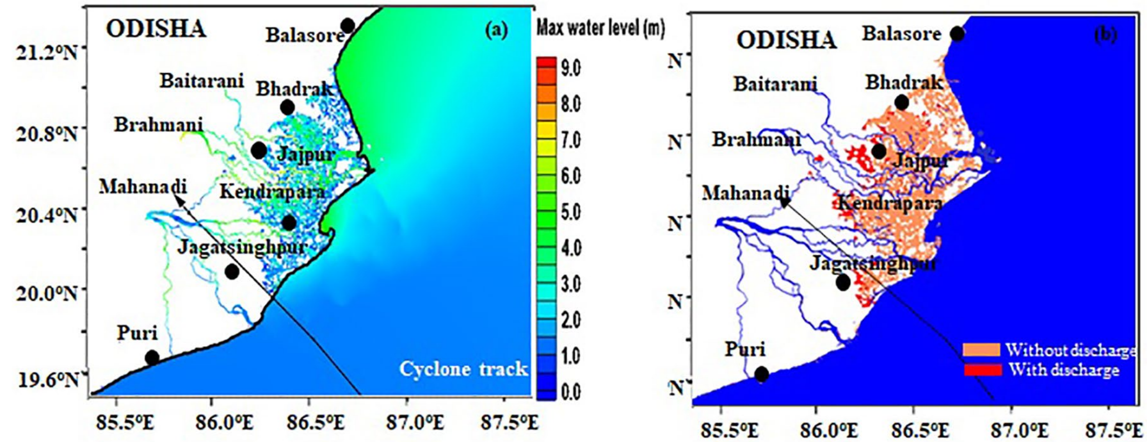

Figure 6. (a) Spatial coverage of coastal inundation and maximum water levels with daily river discharge for the 1999 Super cyclone (b) composite depiction of coastal inundation for 1999 Super cyclone as an aggregate response of without and with discharge.

the 1999 RSMC report as damaged districts and it is also mentioned that severe flooding were seen mainly in Brahmani and Baitarani rivers. However, the information of the extent of inundation is not available in the report.

The enhanced flooding in SIM3 may be caused by the non-linear interaction of the influx from the upstream and ST from the downstream of the river, causing to decrease the penetration of ST into the river channel and resulting in more overbank flooding (Bacopoulos et al., 2017). The inundated area from SIM3 is about 2,275 km^2. It shows that the coastal flooding area is increased by about 14% from SIM1 after incorporating the discharge in the model. On comparison of SIM2 and SIM3, it is observed that the upstream discharge and the proper representation of the river basin have increased the coastal inundated area by about 70% in the case of an extremely severe cyclonic event, which made landfall in the river deltaic region. This infers that not only representation of river systems in the computational domain is significant but also the freshwater discharge through the river upstream is also a dominant factor to map accurate coastal flooding.

The hydrograph of Mahanadi, Brahmani, and Baitarani rivers in Figure 5 shows that the Brahmani River has a maximum discharge of about 8,053 m^3/s. Therefore, to assert the contribution of influx from Brahmani River on the coastal inundation during the 1999 Super cyclone, one more simulation (SIM4) is conducted that is discussed in Appendix B.

In all the above simulations (SIM1, SIM2, SIM3, and SIM4), the LULC data is used to compute spatially varying bottom stress with Manning's n coefficients. For the 1999 Super cyclone, 2000 GLCC LULC data is used, having a resolution of about 1 km. Manning's roughness coefficient (n) is used to model spatially varying bottom stress and is very important as it affects computation of coastal inundation. The major classes of 2000 GLCC LULC in the Mahanadi delta region is shown in Appendix A. Therefore, to investigate the role of the LULC on coastal flooding, an experiment (SIM5) is carried out for the 1999 Super cyclone without using LULC information. The experimental setup in SIM5 is similar to SIM3 except that the bottom stress in SIM5 is computed using hybrid bottom friction formulation with a minimum drag coefficient of 0.0015.

Figure 7a depicts spatial coverage of coastal inundation and MWL from SIM5. The MWL of about 10 m is seen in the river streams, and the inland extent flooding increases in the district of Bhadrak, Kendrapara, Jagatsinghpur, and Jajpur. The extent is about 74 and 60 km near Brahmani and Baitarani rivers, respectively. However, there are no field observations available to validate the inundation extent. Moreover, a composite extent of flooding as a combined response of SIM5 and SIM3 is shown in Figure 7b that highlights an increase in the extent without LULC. The inundated area from SIM5 is about 3,475 km^2, while it is about 2,275 km^2 from SIM3. This suggests that a decrease of about 1,200 km^2 or 35% in the computed inundated area after introducing LULC data in the model. It infers from the simulations that MWL and extent of inundation vary with the use of LULC information. To understand the variation in water depths for each class of LULC, the MWL with LULC is extracted and at the same location without LULC is noted and plotted in

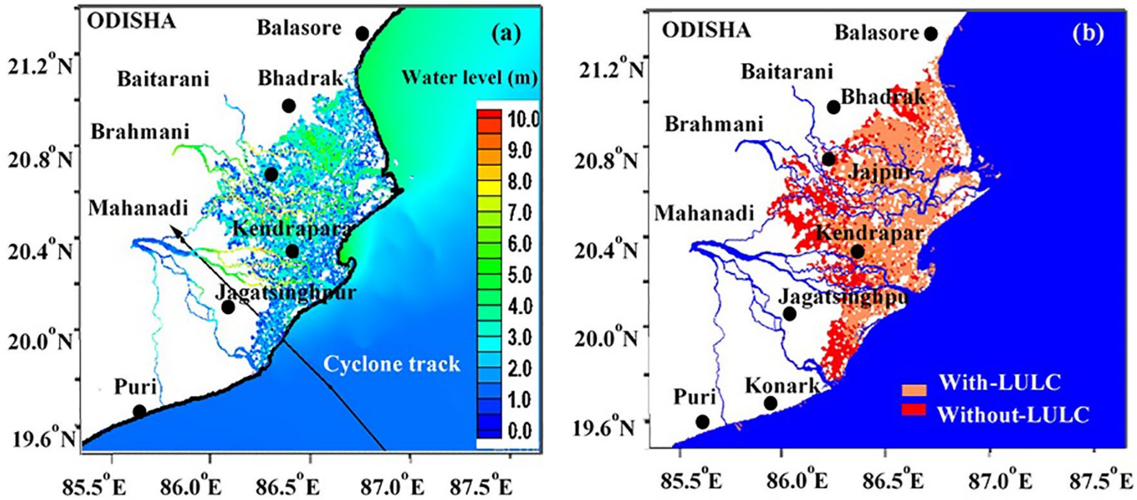

Figure 7. (a) Spatial coverage of coastal inundation and maximum water levels without including land use/land cover (LULC) for 1999 Super cyclone, (b) a composite depiction of coastal inundation as an aggregate response of with and without LULC for 1999 Super cyclone.

Figure 8. It is noticed that there is a significant reduction in MWL with the inclusion of LULC in the model simulations. The settlement, tropical dry deciduous forest, mangroves, water bodies (rivers and lakes), and rain-fed agriculture reduce the MWL with a maximum reduction of 29% with the tropical dry deciduous forest. It is inferred on comparison of SIM3 and SIM5 that the LULC has a significant impact on water depths and flooding extent by acting as a barrier and reducing the flow velocity. Therefore, it is essential to incorporate LULC information to predict the inundation extent accurately during the cyclone period.

5.1.2. Phailin Cyclone

The computation of coastal flooding in the Mahanadi delta is analyzed (SIM3) for the Phailin cyclone, which makes landfall about 100 km south of the Mahanadi river delta region. The delta is on the right side of the cyclone track, and the distance of the track from Puri is about 100 and 270 km from Dhamara. Daily observed freshwater discharge at Tikarapara, Jenapur, and Anandapur during the cyclone period is shown in Figure 9. Maximum discharge of about 15,000 m^3/s is observed at Tikarapara. The model simulated tide is validated at Paradeep tide-gauge station, which is about 200 km right to the landfall location. The validation is carried out for the last 10 days (out of 30 days spin-up period) as shown in Figure 10a. It is observed that the amplitude and phase of the model tide is in good match with the observations, which shows that the model has attained the steady state condition and the correlation coefficient is about 0.98. Similarly, the model computed ST is also validated during the cyclone period with the observations at Paradeep tide-gauge station (Figure 10b). It is found that the simulated ST compares reasonably well with the observations with an RMSE of about 0.22 m.

The spatial distribution of coastal flooding and MWL for the Phailin cyclone is shown in Figure 11. The MWL of about 2.5 m is simulated near Gopalpur, and it is about 5 m in the tributaries of Mahanadi, Brahmani, and Baitarani rivers. Inland inundation is observed in Bhadrak district near the Baitarani River with a covered area of about 75 km^2. It is observed that the extent of flooding in the Mahanadi delta is not significant in the case of the Phailin cyclone. This may be attributed to the fact that the maximum ST simulated near the river mouth varies only from 1 m to about 1.5 m with a minimum near Puri to a maximum near Dhamara.

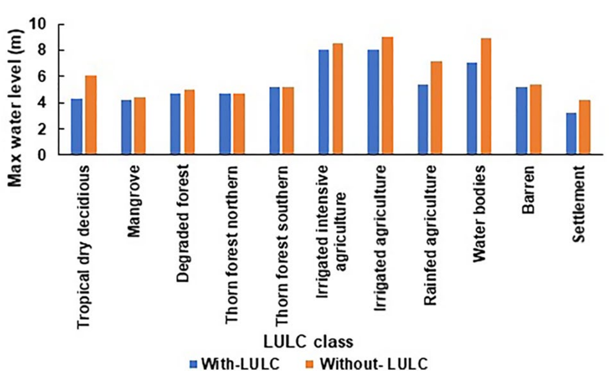

Figure 8. Inundated maximum water levels with and without land use/land cover for each classification in the Mahanadi delta region.

5.2. HEC-RAS Simulations

As mentioned in Section 4.2, the Exp1 and Exp2 are carried out without and with precipitation for both the cyclones. Initially the experiments are

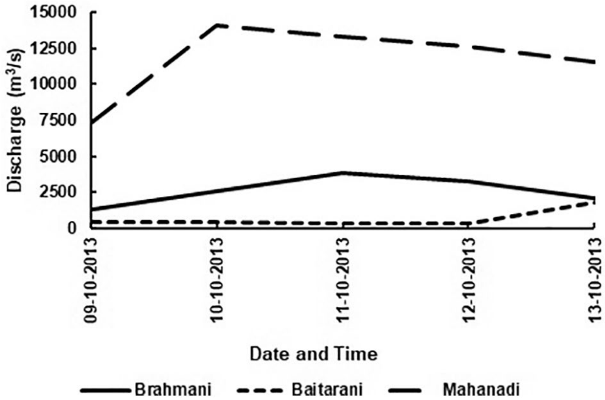

Figure 9. Daily discharge hydrograph during the 2013 Phailin cyclone at Mahanadi, Brahmani and Baitarani.

performed to map flood inundation in the delta region during the Phailin cyclone, which made landfall 100 km south to the Mahanadi delta as a response of ST + RD and ST + RD + P, respectively. The ADCIRC computed temporal ST values provide as downstream boundary condition at Baitarani, Brahmani and the Mahanadi RCB are shown in Appendix A. Figures 12a and 12b depict the MWL and coastal inundation in the delta region for Exp1 and Exp2, respectively. The MWL computed is about 6 m near the Brahmani River (Figure 12a). The inundation is also observed in the coastal districts of Bhadrak and Jajpur and in some places in Kendrapara near Brahmani River.

On comparison of SIM3 (Figure 11) carried out for the Phailin cyclone, it is observed that the inundated area is enhanced in the Exp1. The reason may be due to the changes in the river depth profiles, which are modified in the HEC-RAS model by changing the river bank profile using cross-sections, and that may lead to changes in the water carrying capacity of the rivers. In SIM3, it is observed that only the low-lying areas of Bhadrak are inundated, and as mentioned earlier, the inundation area is about 75 km^2. Whereas, the inundated area computed in Exp1 is about 532 km^2. The inundation of the Jajpur district in the Brahmani River coincides with the peak discharge time of the Brahmani River that is on October 11, 2013 (refer: Figure 9). Moreover, the inundated area in Exp2 (Figure 12b) is about 1,124 km^2 after incorporating daily averaged rainfall along with ST and RD. It is observed that the inundated area is increased by about two times after incorporating P, which may be slightly on the higher side as evaporation and soil infiltration data are not included in the model. The simulated inundation is validated with the image obtained from the Landsat-8 satellite. Figure 12c shows the satellite image of the Mahanadi delta captured on April 26, 2013 when the region was cloud-free and Figure 12d is of October 19, 2013 seven days after the landfall of the cyclone. The modified normalized difference water index (MNDWI) is carried out for both the images to enhance the open water features (Xu, 2006) in the satellite image. As observed in the satellite image (Figure 12d), the model simulations capture reasonably well the inundated areas of Bhadrak and Jajpur, highlighted with a black oval-shaped contour in Figure 12b. However, small inundated areas are not seen in the imagery as mentioned before the image was taken seven days after the cyclone’|’s landfall. Therefore, it is inferred that coupling a hydrodynamic (ADCIRC) model with a hydraulic river system (HEC-RAS) helps to achieve more accurate flood mapping in the river delta regions as the coupled model system can simulate better fluid flows in the estuarine coastal region.

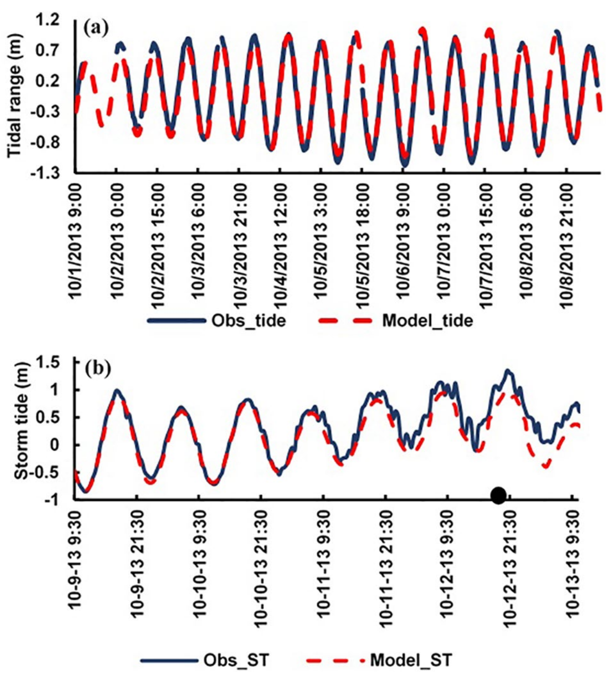

Figure 10. (a) Comparison of modeled tide against the observed tide at Paradeep (20.24°N, 86.64°E), (b) Comparison of model simulated storm tides with observations for Phailin cyclone. Black dot shows the cyclone landfall time.

Similarly, the HEC-RAS model is used to carry out Exp1 and Exp2 for the 1999 Super cyclone. The temporal ST (simulated through ADCIRC) during the cyclone period is provided in Appendix A. Figure 13 depicts the MWL along with coastal inundation for Exp1 and Exp2 during the 1999 Super cyclone. The MWL computed in both the experiments is about 8 m, near the Brahmani River in Jajpur district and also the districts like Kendrapara, Bhadrak are seen inundated (Figure 13a). On comparing Exp1 with SIM3 for the 1999 Super cyclone, it is seen that the Bhadrak and Kendrapara districts are flooded in both the simulations. However, the region near Brahmani River in the Jajpur district is an additional inundated area simulated in Exp1 during the peak discharge time in the Brahmani River during October 30–31, 2013 (refer Figure 5). This highlights that the flood expanded across the river channel during the peak discharge from the river's upstream. In Exp2, it is noted that the Mahanadi delta region is more inundated after including P as the highest area-averaged precipitation of about 216 mm was reported on October 29, 1999 (1 day before the cyclone landfall). The inundated area computed for Exp1 and

10.1029/2020JC016810

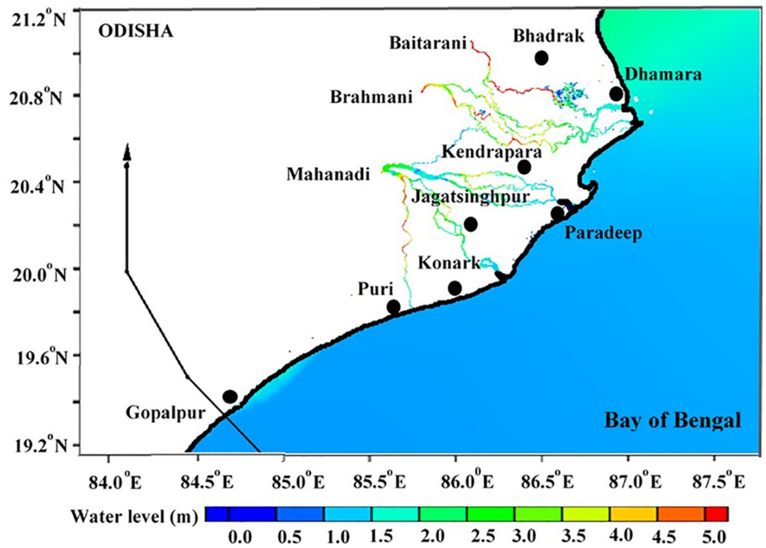

Figure 11. Spatial coverage of coastal inundation and maximum water levels for Phailin cyclone along with cyclone track.

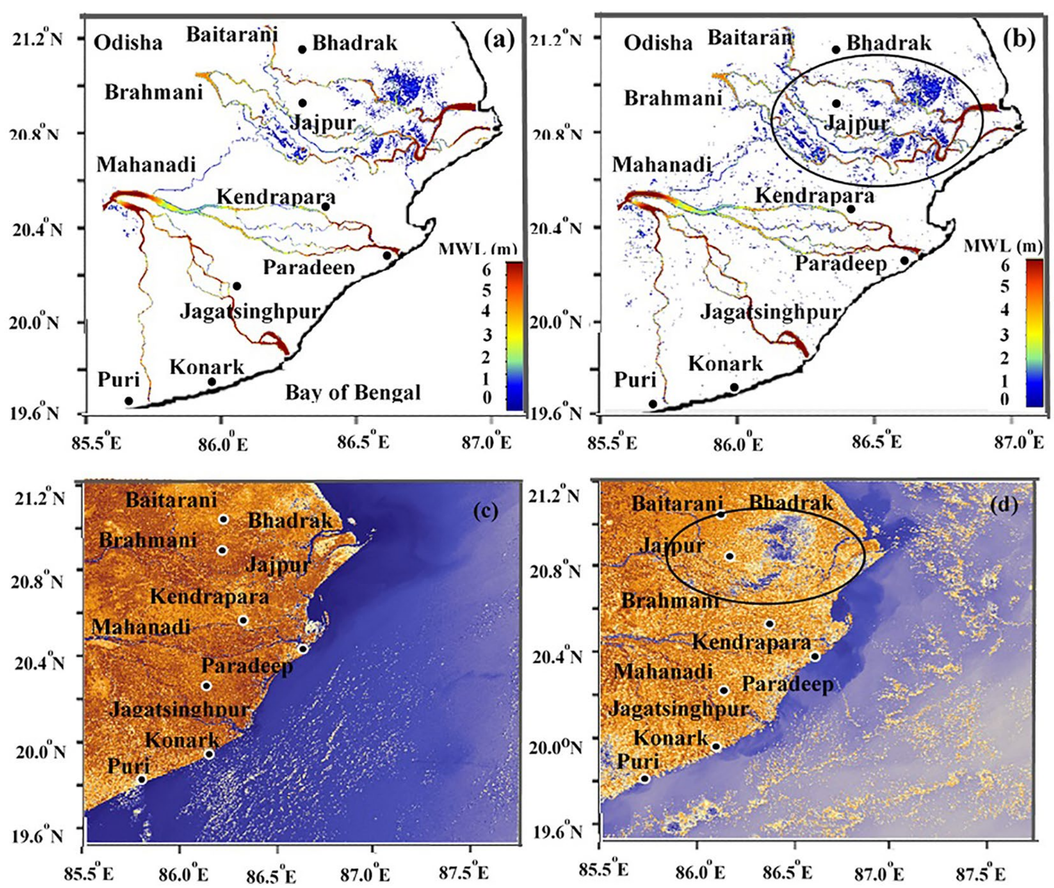

Figure 12. Depiction of maximum water levels and coastal inundation during Phailin cyclone (a) simulation with storm tides and river discharge, (b) simulation with storm tides, river discharge and precipitation. Black oval-shaped highlights the major inundated area, (c) Landsat-8 satellite image of April 26th 2013 when there was no weather system, (d) Landsat-8 satellite image of October 19th 2013 just after the cyclone. Black oval-shaped highlights the major inundated area.

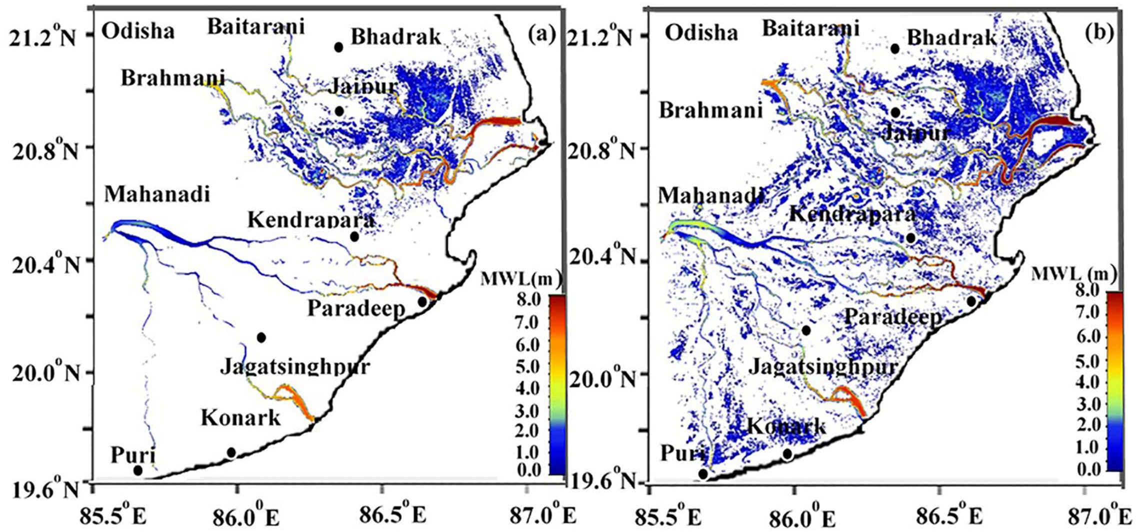

Figure 13. Depiction of maximum water levels and coastal inundation during 1999 Super cyclone (a) simulation with storm tides and river discharge, (b) simulation with storm tides, river discharge and precipitation.

Exp2 is about 1,382 and 2,800 km^2, respectively. This essentially infers again the importance of using the coupled model system with the inclusion of P to map the inland flooding accurately during any cyclonic event.

6. Conclusions

The study emphases on the computation of coastal flooding in the Mahanadi River delta during the cyclone period by incorporating rivers with representative depths and including hydrological components (river discharge and precipitation) in the standalone ADCIRC and coupled ADCIRC and HEC-RAS models. Numerical simulations are performed for the 1999 Super cyclone and the 2013 Phailin cyclone, which made landfall through the delta region and 100 km south of it, respectively. The SRTM data used for the on-shore topography is modified by incorporating the approximated river depths of Mahanadi, Brahmani, and the Baitarani River channels using available river cross-sectional data. A finite element mesh with the normal flux boundary at the upstream of the rivers is generated for the Odisha coast using the merged GEBCO and modified SRTM data.

The coastal flooding is quantified in the delta region during the 1999 Super cyclone using a standalone ADCIRC model with and without modified SRTM data. It is found that the inundated area increases by about 64% after incorporating river streams with approximated depths. Moreover, the contribution of freshwater discharge is estimated using its daily data available from WRIS at the upstream end of the Mahanadi, Brahmani, and Baitarani rivers. The inundated area after incorporating river discharge is expanded by about 14%. The study highlights that it is essential to include hydrological components with proper representation of the river systems in the computational domain in order to map inland inundation precisely due to the cyclone. The effect of river discharge is assessed on the coastal flooding by incorporating the discharge only through the Brahmani River. As the maximum discharge of about 8,053 m^3/s was observed at the upstream of Brahmani River during the 1999 Super cyclone, it is noticed that about 7% is contributed alone by this discharge out of 14% increase in the inundated area.

Similarly, an experiment is made with a hybrid bottom friction formulation with a friction coefficient value of 0.0015 to study the effect of LULC on the coastal flooding. The coastal inundation is reduced by 35% with the LULC, which demonstrates that it is essential to incorporate LULC information in order to compute more reliable inland inundation. Another simulation carried out for the 2013 Phailin cyclone computes an inundated area of only about 75 km^2 in the low-lying areas of Bhadrak district. Moreover, the model computed storm tides is found to be in good agreement with the Paradeep tide-gauge data with an RMSE of about 0.22 m.

The impact of inland precipitation on the computation of inundated area is estimated by using a coupled ADCIRC and HEC-RAS model for the Phailin cyclone and the 1999 Super cyclone. The 2D unsteady HEC-RAS model is configured for the Mahanadi delta region by incorporating ADCIRC computed ST into the downstream RCB and the daily observed discharge in the upstream boundary. Experiments with and without daily area-averaged precipitation are performed for both the cyclones to quantify the effect of precipitation on the inland flooding. For the Phailin cyclone, the coastal flooding without precipitation is computed in the low-lying areas of Bhadrak and also in Jajpur district near Brahmani River with an inundated area of about 534 km^2. Whereas, the inundated area becomes almost double with inland precipitation. The increase may be on the higher side as evaporation and soil infiltration data are not incorporated in the model due to lack of information. The simulated coastal flooding is compared with the Landsat-8 satellite image, which shows a better agreement with the major inundated areas. Similarly, in the 1999 Super cyclone inland precipitation increases the inundated area by about two times.

The study exhibits that a coupled hydrodynamic and hydraulic model system supports to achieve a more reliable flood mapping in the river delta region. Including precipitation along with river discharge have also a large effect on the inundation estimates. This modeling approach has further allowed to understand and quantify the influence of hydrological components and the significance of resolving river systems in the computation of flooding due to an impinging cyclone making landfall into the river delta region or in its vicinity.

Owing to the unavailability of the actual river bathymetry in the public domain, an effort is made in this study to develop a modeling system that assists in understanding the role of river discharge, ST and precipitation in the computation of coastal inundation by incorporating Mahanadi delta with an approximated bathymetry. The present study considers two cyclonic cases which are 15 years apart but due to the limited availability of river cross-sectional data the changes in the river course is not considered. Furthermore, the river bed and its width are not precisely represented at certain locations. This may alter the water carrying capacity of the river and may lead to a misrepresentation of over bank flooding at those locations. However, the system appeared to provide encouraging results after incorporating river discharge and cyclone induced precipitation. Though the study and its results are constrained to the availability of the data along with some uncertainties, it is nevertheless that the system can be utilized and verified with the upcoming cyclonic events. It also provides a platform to improve further by prescription of finer details of the river basin, including spatially distributed rainfall for the computation of inland flooding and eventually validating model computed coastal inundation by ground truth data either in the form of in situ observations or satellite images. The accurate prediction of flood risk would help to enhance the efficacy of the disaster management and mitigation plans.

Appendix A: Classification of Land Cover Characteristics and Corresponding Manning's *n* Values

Table A1 shows Manning's *n* value for different classes of Global Land Cover Characteristics (GLCC) and Bhuvan-National Remote Sensing Center (NSRC) land use/land cover (LULC) data.

The Mahanadi deltaic region of DT-1 (with modified Shuttle Radar Topography Mission (SRTM) data) and DT-2 (with original 30 m SRTM data) is shown in Figure A1. It is evident from the figure that the Mahanadi,

Table A1
Manning's n Values for 2000 GLCC and 2013 NRSC LULC Classes

2000 GLCC LULC classification		NRSC 2013 LULC classification	
Class Description	Manning's *n*	Class Description	Manning's *n*
Sea	0.02	Settlement	0.15
Tropical evergreen	0.32	Kharif crop only	0.03
Subtropical evergreen	0.32	Rabi crop/zaid/double/triple crop	0.04
Temperate broadleaved	0.4	Mixed dryland/irrigation	0.035
Tropical montane	0.6	Current fallow	0.032
Tropical semievergreen	0.16	Crop/wood mosaic	0.042

Table A1
Continued

2000 GLCC LULC classification		NRSC 2013 LULC classification	
Class Description	Manning's n	Class Description	Manning's n
Temperate conifer	0.16	Grassland	0.035
Subtropical conifer	0.16	Scrub/deg. Forest/scrubland	0.4
Tropical moist deciduous	0.32	Mix shrub/Grs	0.05
Tropical dry deciduous	0.32	Savanna	0.16
Junipers	0.435	Deciduous forest	0.36
Mangroves	0.0951	Deciduous needle leaf	0.1
Degraded forest	0.036	Evergreen forest	0.32
Dry woodland	0.055	Evergreen forest (Himalayan region)	0.12
Thorn forest/scrub (northern)	0.4	Plantations/orchard/shifting cultivation	0.1
Thorn forest/scrub (southern)	0.4	Water bodies	0.02
Shrubs	0.1	Herbaceous wetland	0.035
Abandoned jhum	0.1	Littoral swamp (mangrove)	0.0951
Sparse woods	0.1	Other wasteland/gullied/ran	0.0113
Bush	0.1	Herbaceous tundra	0.04
Coastal vegetation	0.035	Wooded tundra	0.05
Savannah	0.16	Mixed tundra	0.05
Plain grasslands	0.035	Bare ground tundra	0.05
Slope grasslands	0.025	Snow cover	0.022
Desert grasslands	0.01		
Alpine meadow	0.025		
Alpine grasslands	0.05		
Sparse vegetation (cold)	0.037		
Sparse vegetation (hot)	0.037		
Gobi	0.037		
Desert (cold)	0.025		
Thorn scrub/desert (hot)	0.1		
Irrigated intensive agriculture	0.035		
Irrigated agriculture	0.035		
Slope agriculture	0.035		
Rainfed agriculture	0.035		
Current jhum	0.1		
Swamp	0.071		
Coral reef	0.3		
Water bodies	0.025		
Snow	0.022		
Barren	0.0113		
Bare rock	0.03		
Salt pans	0.025		
Mud flats	0.041		
Settlement	0.15		

Abbreviation: GLCC, Global Land Cover Characterization; NSRC, Bhuvan-National Remote Sensing Center; LULC, land use/land cover.

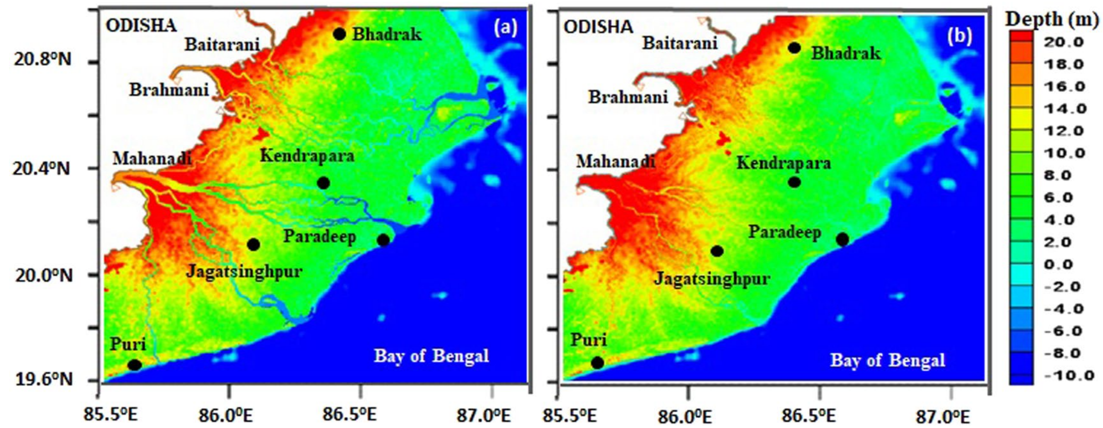

Figure A1. Bathymetry and onshore topography of the Mahanadi deltaic region for the model domain (a) DT-1 (modified Shuttle Radar Topography Mission (SRTM) data) (b) DT-2 (unmodified SRTM data).

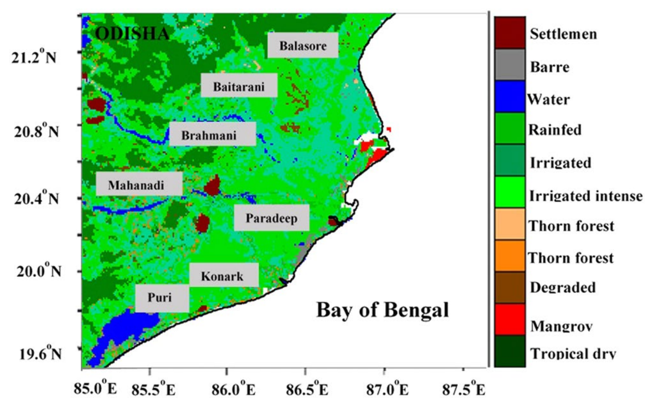

Figure A2. Depiction of land use/land cover data over the Mahanadi delta.

Brahmani, Baitarani rivers and their major tributaries are well represented in the domain with DT-1 (Figure A1a) compared with DT-2 (Figure A1b).

The GLCC LULC, used for the computation of coastal inundation due to the 1999 Super cyclone covers 11 classes of LULC over the Mahanadi delta region with agriculture as the major constituent. Figure A2 depicts the GLCC data over the Mahanadi delta region.

The Advanced Circulation (ADCIRC) computed temporal storm tide (ST) values at the river coastal boundary (RCB) openings of Baitarani, Brahmani, and the Mahanadi River (refer: Figure 3) are shown in Figure A3a–A3e, respectively. These values are provided as the downstream boundary conditions for the Hydrologic Engineering Center River Analysis System (HEC-RAS) model during the Phailin cyclone.

During 1999 Super cyclone temporal values of ADCIRC computed ST, is shown in Figure A4. The maximum ST of about 3.5, 3.2, and 2 m at the time of cyclone landfall is computed near the Brahmani, Baitarani, and Mahanadi rivers, respectively. On comparison, the other two Mahanadi RCB are on the left side of the cyclone track having negative 1.3 and 2.5 m of ST, respectively. These values are provided as downstream boundary condition in the HEC-RAS model for the Exp1 and Exp2 of 1999 Super cyclone.

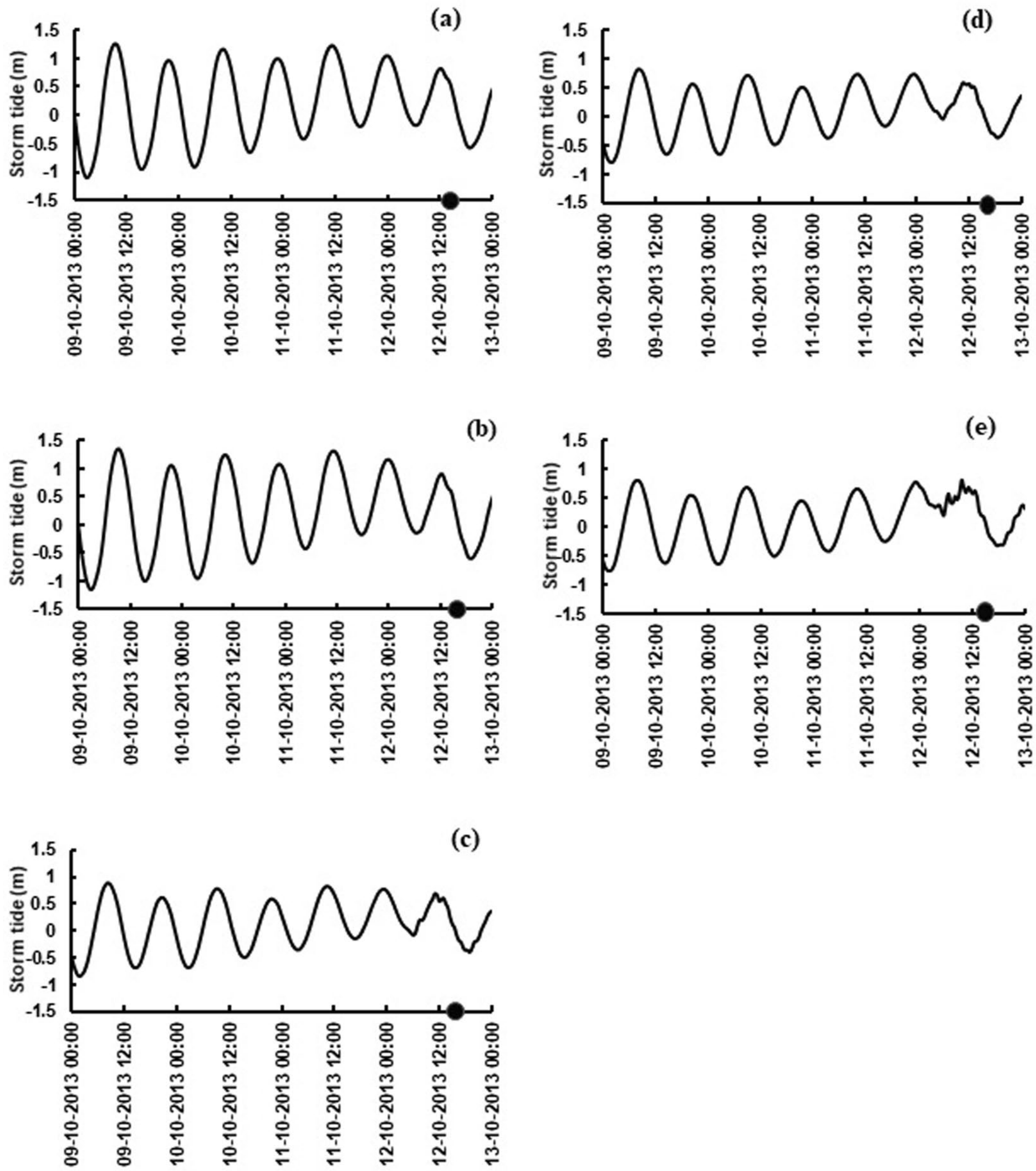

Figure A3. Temporal depiction of storm tides during the Phailin cyclone at river coastal boundary (a) opening1, (b) opening2, (c) opening3, (d) opening4, (e) opening5. Black dot on the *x*-axis represents the cyclone landfall time.

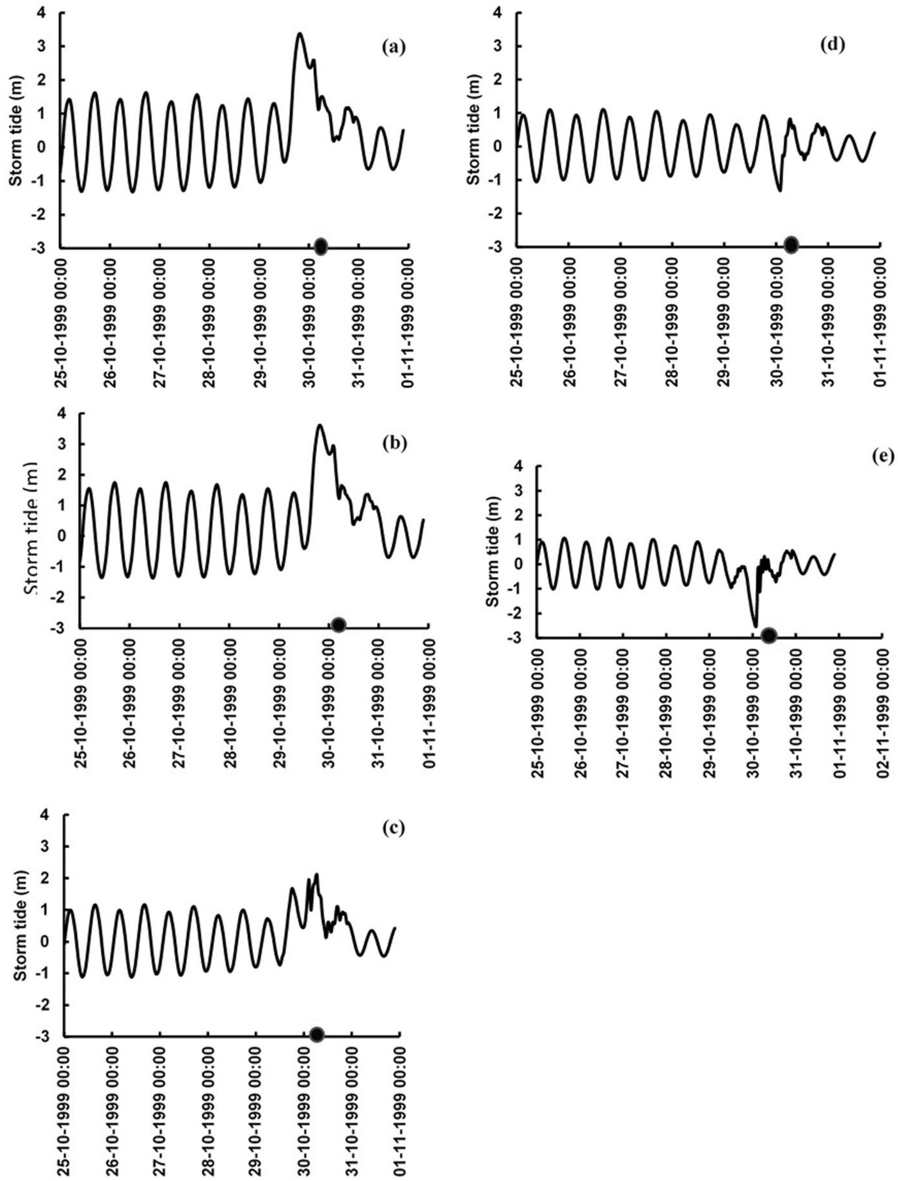

Figure A4. Temporal depiction of storm tides during the 1999 Super cyclone at river coastal boundary (a) opening1, (b) opening2, (c) opening3, (d) opening4, (e) opening5. Black dot on the *x*-axis represents the cyclone landfall time.

Appendix B: SIM4: Simulation to Determine the Role of River Discharge Through Brahmani River

In order to interpret the contribution of the river discharge through Brahmani River alone, SIM4 is carried out. The maximum discharge through the river is about 8,053 m^3/s. This simulation is similar to SIM3 (with discharge through all the three rivers that is Mahanadi, Brahmani and Baitarani rivers) except that discharge is considered only at the upstream of Brahmani River. Whilst, the discharge through Mahanadi and Baitarani is kept zero. A composite depiction of coastal inundation as an aggregate response of SIM1 and SIM4 is shown in Figure B1. It is observed that the extent of inundation increases only in the coastal districts of Jajpur, and the total inundated area in SIM4 is about 2095 km^2 after incorporating discharge only through Brahmani River. This shows that the inundated area increases by 7% from SIM1. It is interesting to note that the increase in the inundated area is about 14% (SIM3) when the discharge is incorporated in all

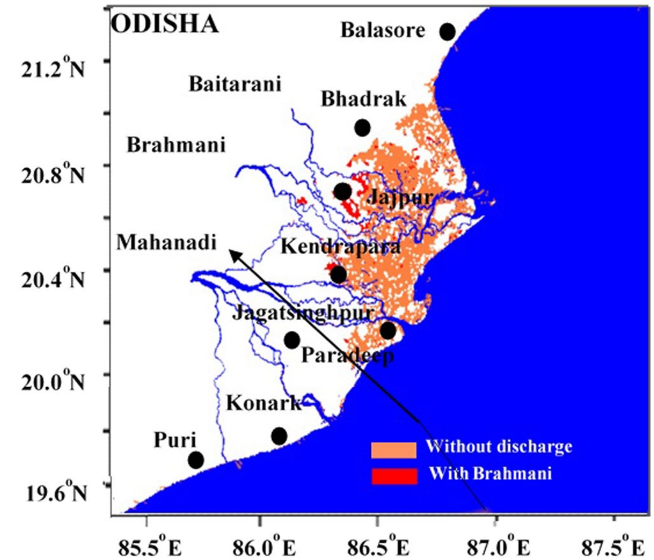

Figure B1. A composite depiction of coastal inundation as an aggregate response of with no-discharge and with discharge only through Brahmani River.

the rivers (Mahanadi, Brahmani, and Baitarani). It is found that, the discharge only through the Brahmani contributes a 7% increase, inferring this river alone pays 50% of the increase in the inundated area.

Appendix C: Sensitivity Experiments on Inundation

(a) Effect of the river width on inundation

Sensitivity experiments are carried out to understand uncertainty associated with the model in computing coastal inundation as the river cross-sectional width changes. These are performed using coupled HEC-RAS and ADCIRC model without precipitation for the 1999 Super cyclone. To make the model set-up simple, the cross-sectional width of only the Baitarani River is reduced by 25% and 50%. Moreover, the upstream discharge is provided only through the Baitarani River, while ADCIRC computed ST are prescribed through the all the RCB of the domain. This experimental set-up assists in quantifying the effect of width change on the inundation area. The flood mapping is initially carried out with no change in Baitarani River width, that is, 0% change. Subsequently, the inundation is compared with the experiments performed for 25% and 50% reduction in width. It is observed that the inundated area increases by about 3% and 15% in response to the reduction of 25% and 50% in the width, respectively. The increase in the flooded area is caused as the water carrying capacity of the river reduces with a reduction in width. Hence, the overbank flooding increases, leading to an increase in the flood plain. Table C1 shows the computed inundated area and its increase in percentage.

Table C1
Computed Inundated Area and Increase in Percentage With Change in River Width

Reduction in river depth (in %)	Computed inundated area (in km^2)	Increase in area over 0% (in %)
0%	856	–
25%	881	3
50%	988	15

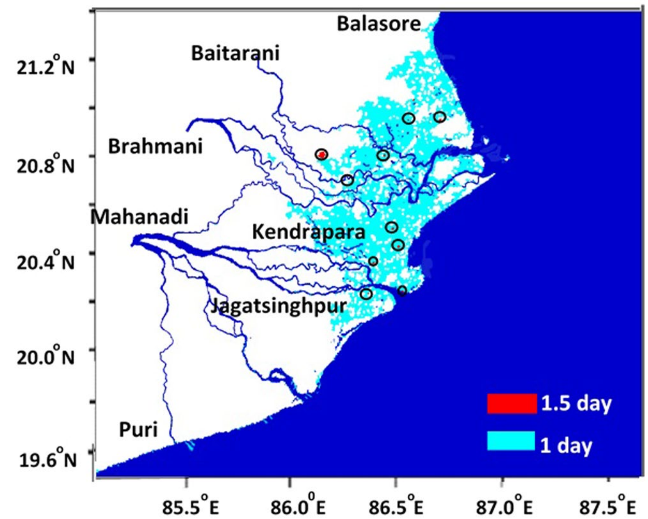

Figure C1. Composite depiction of coastal inundation for 1999 Super cyclone as an aggregate response of 1-day and 1.5-days ramping.

(b) Effect of ramp function on inundation

Experiments are carried out by changing the ramping function from 1-day to 1.5 and 2-days. For this experiment, the model is set-up with prescription of tidal amplitude and corresponding phase of different constituents at the open boundary and daily discharge at the upstream flux boundary of the rivers. The model is run for five days with improved Jelesnianski cyclonic winds for the 1999 Super cyclone and other parameter settings are same as that described in the main manuscript. For the ramping of 1-day, the computed coastal inundation for the 1999 Super cyclone is the same as shown in Figure 7a of the main text and the corresponding calculated inundated area is about 2,275 km^2 as mentioned in the manuscript (ref: Line no. 540). While, the inundated area is increased only by 13 km^2 (that is about 0.5% of the increase) when the ramping function is changed to 1.5-days. A composite depiction of coastal inundation as an aggregate response of 1-day and 1.5-days is shown below in Figure C1. The red color in the figures (inside the black circle) shows the extra inundated area for 1.5-days and the light blue color shows the area for 1-day. However, the inundated area is reduced to about 2,243 km^2 (i.e., a decrease of about 1.4%) for 2 days ramping, which means

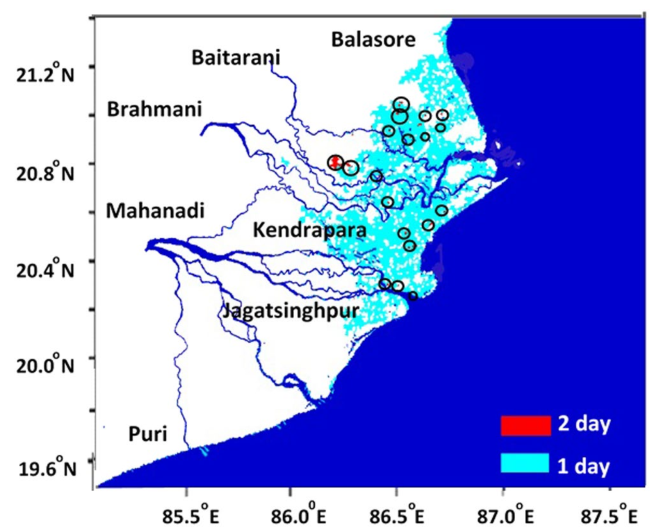

Figure C2. Composite depiction of coastal inundation for 1999 Super cyclone as an aggregate response of 1-day and 2-days ramping.

an extra inundated area of about 32 km^2 for 1-day ramping is computed as shown in Figure C2, which is also a composite depiction of coastal inundation as an aggregate response of 2-days and 1-day ramping. Red color (inside black circle) in the figure depicts the additional area inundated with 1-day ramping. These experiments suggest that computation of the inundated area is unaltered considerably in response to use of different ramping days in the model.

Data Availability Statement

The best track data can be obtained from the IMD site (http://www.rsmcnewdelhi.imd.gov.in/index.php?option=com_content&view=article&id=48&Itemid=194&lang=en). Data sets for this research are available through Pandey (2020a, 2020b).

Acknowledgments

The authors are thankful to the Indian National Center for Ocean Information Service for providing tide gauge data, the India Meteorological Department for providing best track data and rainfall data and Water Resources Information System for river discharge data set. Thanks are also due to the Indian Institute of Technology Delhi HPC facility and Department of Science and Technology, Government of India in sanctioning financial grant (DST-FIST, 2014) for computational resources.

References

Agnihotri, N., Chittibabu, P., Jain, I., Sinha, P. C., Rao, A. D., & Dube, S. K. (2006). A bay–river coupled model for storm surge prediction along the Andhra coast of India. *Natural Hazards*, *39*(1), 83–101. https://doi.org/10.1007/s11069-005-3812-7

Atkinson, J. H., Westerink, J. J., & Luettich, R. A., Jr. (2004). Two-dimensional dispersion analyses of finite element approximations to the shallow water equations. *International Journal for Numerical Methods in Fluids*, *45*(7), 715–749. https://doi.org/10.1002/fld.701

Bacopoulos, P., Tang, Y., Wang, D., & Hagen, S. C. (2017). Integrated hydrologic-hydrodynamic modeling of estuarine-riverine flooding: 2008 Tropical Storm Fay. *Journal of Hydrologic Engineering*, *22*(8), 04017022. https://doi.org/10.1061/(asce)he.1943-5584.0001539

Beardsley, R. C., Chen, C., & Xu, Q. (2013). Coastal flooding in Scituate (MA): A FVCOM study of the 27 December 2010 nor'easter. *Journal of Geophysical Research: Oceans*, *118*(11), 6030–6045. https://doi.org/10.1002/2013jc008862

Bhaskaran, P. K., Nayak, S., Bonthu, S. R., Murty, P. N., & Sen, D. (2013). Performance and validation of a coupled parallel ADCIRC–SWAN model for THANE cyclone in the Bay of Bengal. *Environmental Fluid Mechanics*, *13*(6), 601–623. https://doi.org/10.1007/s10652-013-9284-5

Blain, C. A., Westerink, J. J., & Luettich, R. A., Jr. (1994). The influence of domain size on the response characteristics of a hurricane storm surge model. *Journal of Geophysical Research*, *99*(C9), 18467–18479. https://doi.org/10.1029/94jc01348

Bricker, J. D., Gibson, S., Takagi, H., & Imamura, F. (2015). On the need for larger Manning's roughness coefficients in depth-integrated tsunami inundation models. *Coastal Engineering Journal*, *57*(02), 1550005. https://doi.org/10.1142/s0578563415500059

Brunner, G. W. (2002). HEC-RAS (river analysis system). In *North American water and environment congress & destructive water* (pp. 3782-3787). ASCE.

Bunya, S., Dietrich, J. C., Westerink, J. J., Ebersole, B. A., Smith, J. M., Atkinson, J. H., et al. (2010). A high-resolution coupled riverine flow, tide, wind, wind wave, and storm surge model for southern Louisiana and Mississippi. Part I: Model development and validation. *Monthly Weather Review*, *138*(2), 345–377. https://doi.org/10.1175/2009mwr2906.1

Chittibabu, P., Dube, S. K., Macnabb, J. B., Murty, T. S., Rao, A. D., Mohanty, U. C., & Sinha, P. C. (2004). Mitigation of flooding and cyclone hazard in Orissa, India. *Natural Hazards*, *31*(2), 455–485. https://doi.org/10.1023/b:nhaz.0000023362.26409.22

Cyriac, R., Dietrich, J. C., Fleming, J. G., Blanton, B. O., Kaiser, C., Dawson, C. N., & Luettich, R. A. (2018). Variability in Coastal Flooding predictions due to forecast errors during Hurricane Arthur. *Coastal Engineering*, *137*, 59–78. https://doi.org/10.1016/j.coastaleng.2018.02.008

Dawson, C., Westerink, J. J., Feyen, J. C., & Pothina, D. (2006). Continuous, discontinuous and coupled discontinuous–continuous Galerkin finite element methods for the shallow water equations. *International Journal for Numerical Methods in Fluids*, *52*(1), 63–88. https://doi.org/10.1002/fld.1156

Dietrich, J. C., Kolar, R. L., & Luettich, R. A. (2004). Assessment of ADCIRC's wetting and drying algorithm. In Developments in water science (Vol. 55, pp. 1767-1778). Elsevier. https://doi.org/10.1016/s0167-5648(04)80183-7

Dietrich, J. C., Zijlema, M., Westerink, J. J., Holthuijsen, L. H., Dawson, C., Luettich, R. A., Jr., et al. (2011). Modeling hurricane waves and storm surge using integrally-coupled, scalable computations. *Coastal Engineering*, *58*(1), 45–65. https://doi.org/10.1016/j.coastaleng.2010.08.001

Dresback, K. M., Fleming, J. G., Blanton, B. O., Kaiser, C., Gourley, J. J., Tromble, E. M., et al. (2013). Skill assessment of a real-time forecast system utilizing a coupled hydrologic and coastal hydrodynamic model during Hurricane Irene (2011). *Continental Shelf Research*, *71*, 78–94. https://doi.org/10.1016/j.csr.2013.10.007

Dube, S. K., Sinha, P. C., Rao, A. D., Jain, I., & Agnihotri, N. (2005). Effect of the Mahanadi River on the development of storm surge along the Orissa coast of India: A numerical study. *Pure and Applied Geophysics*, *162*(8), 1673–1688. https://doi.org/10.1007/s00024-005-2688-5

Farr, T. G., Rosen, P. A., Caro, E., Crippen, R., Duren, R., Hensley, S., & Alsdorf, D. (2007). The shuttle radar topography mission. *Reviews of Geophysics*, *45*(2), RG2004. https://doi.org/10.1029/2005rg000183

Gayathri, R., Bhaskaran, P. K., & Murty, P. L. N. (2019). River-tide-storm surge interaction characteristics for the Hooghly estuary, East coast of India. *ISH Journal of Hydraulic Engineering*, 1–13. https://doi.org/10.1080/09715010.2019.1601036

Georgas, N., Yin, L., Jiang, Y., Wang, Y., Howell, P., Saba, V., et al. (2016). An open-access, multi-decadal, three-dimensional, hydrodynamic hindcast dataset for the Long Island Sound and New York/New Jersey Harbor Estuaries. *Journal of Marine Science and Engineering*, *4*(3), 48. https://doi.org/10.3390/jmse4030048

IMD (2018). Report on cyclonic disturbances over north Indian ocean during 2018. http://www.rsmcnewdelhi.imd.gov.in/images/pdf/publications/annual-rsmc-report/rsmc-2018.pdf

Jelesnianski, C. P., & Taylor, A. D. (1973). A preliminary view of storm surges before and after storm modifications. NOAA Technical Memorandum, Environmental Research Laboratories, Weather Modification Program Office-3, p. 33.

Kalsi, S. R., & Srivastava, K. B. (2006). Characteristic features of Orissa super cyclone of 29th October, 1999 as observed through CDR Paradip. *Mausam*, *57*(1), 21.

Kalyanapu, A. J., Burian, S. J., & McPherson, T. N. (2009). Effect of land use-based surface roughness on hydrologic model output. *Journal of Spatial Hydrology*, *9*(2), 51–71.

Kinnmark, I. (1986). Implicit methods. In *The shallow water wave equations: Formulation, analysis and application* (pp. 96-114). Springer, Berlin, Heidelberg. https://doi.org/10.1007/978-3-642-82646-7_6

Kolar, R. L., Westerink, J. J., Cantekin, M. E., & Blain, C. A. (1994). Aspects of nonlinear simulations using shallow-water models based on the wave continuity equation. *Computers & Fluids*, *23*(3), 523–538. https://doi.org/10.1016/0045-7930(94)90017-5

Kumar, K. V., & Bhattacharya, A. (2003). Geological evolution of Mahanadi delta, Orissa using high resolution satellite data. *Current Science*, *85*(10), 1410–1412.

Luettich, R. A., & Westerink, J. J. (2004). *Formulation and numerical implementation of the 2D/3D ADCIRC finite element model version 44. XX* (p. 74). R. Luettich.

Luettich, R. A., Westerink, J. J., & Scheffner, N. W. (1992). ADCIRC: An advanced three-dimensional circulation model for shelves, coasts, and estuaries. Report 1, Theory and methodology of ADCIRC-2DD1 and ADCIRC-3DL.

Mohapatra, M., & Sharma, M. (2015). Characteristics of surface wind structure of tropical cyclones over the north Indian Ocean. *Journal of Earth System Science*, *124*(7), 1573–1598. https://doi.org/10.1007/s12040-015-0613-6

Murty, P. L. N., Sandhya, K. G., Bhaskaran, P. K., Jose, F., Gayathri, R., Nair, T. B, et al. (2014). A coupled hydrodynamic modeling system for PHAILIN cyclone in the Bay of Bengal. *Coastal Engineering*, *93*, 71–81. https://doi.org/10.1016/j.coastaleng.2014.08.006

Pai, D. S., Sridhar, L., Rajeevan, M., Sreejith, O. P., Satbhai, N. S., & Mukhopadhyay, B. (2014). Development of a new high spatial resolution (0.25× 0.25) long period (1901–2010) daily gridded rainfall data set over India and its comparison with existing data sets over the region. *Mausam*, *65*(1), 1–18.

Pandey, S. (2020a). River discharge data, Mendeley Data, V1. https://doi.org/10.17632/mdvzh7prjz.1

Pandey, S. (2020b). Best track data, Mendeley Data, V1. https://doi.org/10.17632/xyd7r5j8df.1

Pandey, S., & Rao, A. D. (2018). An improved cyclonic wind distribution for computation of storm surges. *Natural Hazards*, *92*(1), 93–112. https://doi.org/10.1007/s11069-018-3193-3

Pandey, S., & Rao, A. D. (2019). Impact of approach angle of an impinging cyclone on generation of storm surges and its interaction with tides and wind waves. *Journal of Geophysical Research: Oceans*, *124*(11), 7643–7660. https://doi.org/10.1029/2019jc015433

Pasquier, U., He, Y., Hooton, S., Goulden, M., & Hiscock, K. M. (2019). An integrated 1D–2D hydraulic modeling approach to assess the sensitivity of a coastal region to compound flooding hazard under climate change. *Natural Hazards*, *98*(3), 915–937. https://doi.org/10.1007/s11069-018-3462-1

Passeri, D., Hagen, S. C., Smar, D., Alimohammadi, N., Risner, A., & White, R. (2011). Sensitivity of an ADCIRC tide and storm surge model to Manning's *n*. In *Estuarine and Coastal Modeling (2011)* (pp. 457–475).

Patel, D. P., Ramirez, J. A., Srivastava, P. K., Bray, M., & Han, D. (2017). Assessment of flood inundation mapping of Surat city by coupled 1D/2D hydrodynamic modeling: A case application of the new HEC-RAS 5. *Natural Hazards*, *89*(1), 93–130. https://doi.org/10.1007/s11069-017-2956-6

Peng, M., Xie, L., & Pietrafesa, L. J. (2004). A numerical study of storm surge and inundation in the Croatan–Albemarle–Pamlico Estuary System. *Estuarine, Coastal and Shelf Science*, *59*(1), 121–137. https://doi.org/10.1016/j.ecss.2003.07.010

Phillips, J. V., & Tadayon, S. (2006). *Selection of Manning's roughness coefficient for natural and constructed vegetated and non-vegetated channels, and vegetation maintenance plan guidelines for vegetated channels in central Arizona*. US Geological Survey.

Poulose, J., Rao, A. D., & Bhaskaran, P. K. (2018). Role of continental shelf on non-linear interaction of storm surges, tides and wind waves: An idealized study representing the west coast of India. *Estuarine, Coastal and Shelf Science*, *207*, 457–470. https://doi.org/10.1016/j.ecss.2017.06.007

Provost, Le, C., Lyard, F., Molines, J. M., Genco, M. L., & Rabilloud, F. (1998). A hydrodynamic ocean tide model improved by assimilating a satellite altimeter-derived data set. *Journal of Geophysical Research*, *103*(C3), 5513–5529. https://doi.org/10.1029/97jc01733

Quirogaa, V. M., Kurea, S., Udoa, K., & Manoa, A. (2016). Application of 2D numerical simulation for the analysis of the February 2014 Bolivian Amazonia flood: Application of the new HEC-RAS version 5. *Ribagua*, *3*(1), 25–33. https://doi.org/10.1016/j.riba.2015.12.001

Rao, A. D., Murty, P. L. N., Jain, I., Kankara, R. S., Dube, S. K., & Murty, T. S. (2013). Simulation of water levels and extent of coastal inundation due to a cyclonic storm along the east coast of India. *Natural Hazards*, *66*(3), 1431–1441. https://doi.org/10.1007/s11069-012-0193-6

Rao, A. D., Upadhaya, P., Ali, H., Pandey, S., & Warrier, V. (2020). Coastal inundation due to tropical cyclones along the east coast of India: An influence of climate change impact. *Natural Hazards*, *101*(1), 39–57. https://doi.org/10.1007/s11069-020-03861-9

Ray, T., Stepinski, E., Sebastian, A., & Bedient, P. B. (2011). Dynamic modeling of storm surge and inland flooding in a Texas coastal floodplain. *Journal of Hydraulic Engineering*, *137*(10), 1103–1110. https://doi.org/10.1061/(asce)hy.1943-7900.0000398

RSMC (1999). http://www.rsmcnewdelhi.imd.gov.in/images/pdf/archive/rsmc/1999.pdf

RSMC (2013). http://www.rsmcnewdelhi.imd.gov.in/images/pdf/archive/bulletins/2013/RPHA.pdf

Shankar, C. G., Behera, M. R., & Vethamony, P. (2019). Sensitivity study of wind drag coefficient on surge modelling for tropical cyclone. In *Proceedings of the Fourth International Conference in Ocean Engineering (ICOE2018)* (pp. 813–827), Singapore. Springer. https://doi.org/10.1007/978-981-13-3119-0_54

Sharma, M., & Mohapatra, M. (2017). Standard operation procedure for tropical cyclone vital parameters over North Indian Ocean. In *Tropical cyclone activity over the North Indian Ocean* (pp. 367–381), Cham. Springer. https://doi.org/10.1007/978-3-319-40576-6_24

Singh, D. S. (Ed.) (2017). *The Indian rivers: Scientific and socio-economic aspects*. Springer.

Sinha, P. C., Jain, I., Bhardwaj, N., Rao, A. D., & Dube, S. K. (2008). Numerical modeling of tide-surge interaction along Orissa coast of India. *Natural Hazards*, *45*(3), 413–427. https://doi.org/10.1007/s11069-007-9176-4

Tromble, E., Kolar, R., Dresback, K., Hong, Y., Vieux, B., Luettich, R., & Cooten, Van, S. (2010). Aspects of coupled hydrologic-hydrodynamic modeling for coastal flood inundation. In *Estuarine and Coastal Modeling (2009)* (pp. 724–743).

Tromble, E., Kolar, R., Dresback, K., & Luettich, R. (2013). River flux boundary considerations in a coupled hydrologic-hydrodynamic modeling system. In *Estuarine and Coastal Modeling (2011)* (pp. 510–527).

USACE (2016). *HEC-RAS river analysis system user's manual version 5*. US Army Corps of Engineers. http://www.hec.usace.army.mil/software/hec-ras/documentation/HEC-RAS%205.0%20Users%20 manual.pdf

Van Cooten, S., Kelleher, K. E., Howard, K., Zhang, J., Gourley, J. J., Kain, J. S., et al. (2011). The CI-FLOW project: A system for total water level prediction from the summit to the sea. *Bulletin of the American Meteorological Society*, *92*(11), 1427–1442. https://doi.org/10.1175/2011bams3150.1

Vozinaki, A. E. K., Morianou, G. G., Alexakis, D. D., & Tsanis, I. K. (2017). Comparing 1D and combined 1D/2D hydraulic simulations using high-resolution topographic data: A case study of the Koiliaris basin, Greece. *Hydrological Sciences Journal*, *62*(4), 642–656. https://doi.org/10.1080/02626667.2016.1255746

Wamsley, T. V., Cialone, M. A., Smith, J. M., Ebersole, B. A., & Grzegorzewski, A. S. (2009). Influence of landscape restoration and degradation on storm surge and waves in southern Louisiana. *Natural Hazards*, *51*(1), 207–224. https://doi.org/10.1007/s11069-009-9378-z

Weatherall, P., Marks, K. M., Jakobsson, M., Schmitt, T., Tani, S., Arndt, J. E., et al. (2015). A new digital bathymetric model of the world's oceans hydraulic roughness coefficients for native rangelands. *Earth and Space Science*, *2*(8), 331–345. https://doi.org/10.1002/2015EA000107

Weltz, M. A., Arslan, A. B., & Lane, L. J. (1992). Hydraulic roughness coefficients for native rangelands. *Journal of Irrigation and Drainage Engineering*, *118*(5), 776–790. https://doi.org/10.1002/2015ea000107

Westerink, J. J., Luettich, R. A., Baptists, A. M., Scheffner, N. W., & Farrar, P. (1992). Tide and storm surge predictions using finite element model. *Journal of Hydraulic Engineering*, *118*(10), 1373–1390. https://doi.org/10.1061/(asce)0733-9429(1992)118:10(1373)

Westerink, J. J., Luettich, R. A., Feyen, J. C., Atkinson, J. H., Dawson, C., Roberts, H. J., et al. (2008). A basin-to channel-scale unstructured grid hurricane storm surge model applied to southern Louisiana. *Monthly Weather Review*, *136*(3), 833–864. https://doi.org/10.1175/2007mwr1946.1

Xu, H. (2006). Modification of normalised difference water index (NDWI) to enhance open water features in remotely sensed imagery. *International Journal of Remote Sensing*, *27*(14), 3025–3033. https://doi.org/10.1080/01431160600589179

Zheng, F., Westra, S., & Sisson, S. A. (2013). Quantifying the dependence between extreme rainfall and storm surge in the coastal zone. *Journal of Hydrology*, *505*, 172–187. https://doi.org/10.1016/j.jhydrol.2013.09.054